SAMER AL-REFAI

EVALUATION OF PHOTOVOLTAIC STRUCTURES RECONFIGURATION METHODS

NEU 2016

EVALUATION OF PHOTOVOLTAIC STRUCTURES RECONFIGURATION METHODS

A THESIS SUBMITTED TO THE GRADUATE SCHOOL OF APPLIED SCIENCES

OF

NEAR EAST UNIVERSITY

By
SAMER M . MOHAMEDALI AL REFAI

In Partial Fulfilment of the Requirements for

the Degree of Master of Science

in

Electrical and Electronic Engineering

NICOSIA, 2016

EVALUATION OF PHOTOVOLTAIC STRUCTURES RECONFIGURATION METHODS

A THESIS SUBMITTED TO THE GRADUATE SCHOOL OF APPLIED SCIENCES

OF

NEAR EAST UNIVERSITY

By
SAMER M . MOHAMEDALI AL REFAI

In Partial Fulfilment of the Requirements for

the Degree of Master of Science

in

Electrical and Electronic Engineering

NICOSIA, 2016

SAMER AL-REFAI: EVALUATION OF PHOTOVOLTAIC STRUCTURES RECONFIGURATION METHODS

Approval of Director of Graduate School of Applied Sciences

Prof. Dr. İlkay SALİHOĞLU

We certify this thesis is satisfactory for the award of the degree of Masters of Science in

Electrical and Electronic Engineering

Examining Committee in Charge:

I hereby declare that all information in this document has been obtained and presented in accordance with academic rules and ethical conduct. I also declare that, as required by these rules and conduct, I have fully cited and referenced all material and results that are not original to this work.

Name, Last name: Samer AL-REFAI

Signature:

Date:

ACKNOWLEDGEMENTS

I would like to express my sincere appreciation and thanks to my supervisor, Assoc. Prof. Dr. Mehmet Timur Aydemir, for his guidance and mentorship during my graduate studies.

I would also like to express my deepest gratitude to my parents, my wife, my brothers, sisters, and my children, to whom I would sacrifice my life. I thank them for their love and support during all stages of my life.

Last but not least, I would like to express all my sincere feelings to my friends and university colleagues for the times we have spent together. I also express my deep feelings to the Professors, doctors and staff members at Near East University for their continuous support.

To my parents and family….

ABSTRACT

The last two decades have witnessed a great revolution in the industry of green energy resources. With the development in the manufacturing of high efficiency solar panels; in addition to the advances in the fields of semiconductor industry and DSP production, the renewable energy sources have become easily harvested. However, after these great steps in moving toward the use of clean electrical energy as one of the solutions for the environment pollution, more research started to concentrate on the efficiency of renewable energy capturing. The concentration was pointed in two main directions to increase the harvesting efficiency. These are the maximum power point tracking (MPPT) algorithms and the development of dynamically configurable solar energy structures. While MPPT algorithms guarantee the maximum power point operation in normal and balance conditions, the dynamic configuration structures offer the possibility to avoid losses and problems related to the partial shading of solar structures.

This work focuses on the study of solar systems structures and some PV reconfiguration algorithms. These algorithms have been tested in concordance with suitable MPPT algorithms to evaluate their function and efficiency. Simulation of these algorithms has been carried out using MATLAB/SIMULINK and results are presented and discussed.

Keywords: Solar energy; MPPT; Solar cell; PV reconfiguration; Partial shading; hill climbing techniques

ÖZET

Yeşil enerji kaynakları son yirmi yıl büyük bir devrim geçirmektedir. Yüksek verimli güneş panellerinin üretimindeki gelişmeler ve yarıiletken endüstrisinde ve DSP üretiminde yaşanan ilerlemelerle yenilenebilir enerji kaynaklarından enerji üretimi kolaylaşmıştır. Temiz enerji kaynaklarının çevre kirliliği sorununun çözümü için atılan büyük adımlardan sonra yenilenebilir enerji kaynaklarından enerji üretiminin verimi üzerine yapılan araştırmalar artmıştır. Enerji üretiminin verimini arttırma çalışmaları iki konuda yoğunlaşmıştır. Bu alanlar maksimum güç noktasını izleme (MGNİ) algoritmaları ve dinamik olarak bağlantı değişikliği yapılabilen güneş enerjisi sistemleridir. MGNİ algoritmaları normal ve dengeli çalışma koşullarında maksimum gücün elde edildiği noktada çalışmayı garanti ederken, dinamik olarak bağlantı değişikliği yapılabilmesi kayıpların azaltılması ve kısmi gölgelenmeden kaynaklanan problemleri engellemeye yöneliktir.

Bu çalışma güneş enerjisi sistemleri ve PV panellerin bağlantılarının dinamik olarak yeniden yapılandırılma algoritmaları üzerine yoğunlaşmıştır. Bu algoritmaların işlevselliğini ve etkinliğini değerlendirmek için uygun MGNİ algoritmaları ile testler yapılmıştır. Benzetimle MATLAB SIMULINK ile gerçekleştirilmiş ve elde edilen sonuçlar tartışılmıştır.

Anahtar Kelimeler: Güneş enerjisi; Maksimum Güç Noktası İzleme; Güneş hücresi; PV rekonfigürasyonu; Tepe tırmanma tekniği

TABLE OF CONTENTS

ACKNOWLEDGEMENTS .... **II**

ABSTRACT .... **IV**

ÖZET .... **V**

TABLE OF CONTENTS .... **VI**

LIST OF TABLES .... **VIII**

LIST OF FIGURES .... **IX**

LIST OF ABBREVIATIONS .... **XI**

CHAPTER 1 : INTRODUCTION **1**

1.1 Introduction 1
1.2 Literature Review 3
1.3 Scope and Methods 6

CHAPTER 2: MODELLING OF SOLAR CELL **7**

2.1 Introduction 7
2.2 Equivalent Circuit of the Solar Cell 9
2.3 Types of Solar Modules 12
2.3.1 Mono-crystalline cells 12
2.3.2 Poly-crystalline cells 13
2.3.3 Thin film solar cells 13

CHAPTER 3: RECONFIGURATION OF SOLAR SYSTEMS **18**

3.1 PV Configurations (Interconnection Schemes) 19
3.1.1 Bypassing diode as partial shading solution 20
3.1.2 Irradiance equalization method 22
3.1.3 Dynamic electrical scheme configuration 23
3.1.3.1 Reconfiguration algorithm 25
3.1.3.2 Process of finding the best configuration 26
3.1.4 Adaptive reconfiguration (adaptive banking) method 27
3.1.4.1 Algorithm 1 28
3.1.4.2 Algorithm 2 30

CHAPTER 4: RESULTS AND DISCUSSIONS 34

4.1 Effect of Partial Shading on the Solar Production 34

4.1.1 Equally distributed irradiation, case 1 35

4.1.2 Partial shading of one column of the matrix, case 2 36

4.1.3 Partial shading of horizontal line of the PV matrix, case 3 37

4.1.4 Partial shading of triangular group of elements, case 4 38

4.2 Reconfiguration of PV Matrix 39

4.2.1 Partial shading of one column of the matrix, case 2 40

4.2.2 Partial shading of horizontal line of the PV matrix, case 3 40

4.2.3 Partial shading of triangular group of elements, case 4 41

4.3 Adaptive Bank Reconfiguration 42

4.3.1 Simulation results of adaptive bank 44

4.3.2 First configuration 44

4.3.3 Second configuration 45

4.3.4 Third configuration 46

4.3.5 Conclusions 49

REFERENCES 50

APPENDIX: PARAMETERS OF THE SIMULATED SOLAR PANEL…………....54

LIST OF TABLES

Table 4.1: Parameters of the PV panels 34

Table 4.2 : Different shading parameters of the simulated system 35

Table 4.3: Irradiation scheme of the first configuration 44

Table 4.4: Irradiation scheme of the second configuration... 45

Table 4.5: Irradiation of the solar array, third configuration 47

Table 4.6: Advantages and disadvantages of the different algorithms presented…………45

LIST OF FIGURES

Figure 2.1: Solar cell's structure and components (Barron & Chatelain, 2011). 8
Figure 2.2: Principle of solar cells (Linvents, 2015). 9
Figure 2.3: Equivalent circuit model of a solar cell.. 10
Figure 2.4: Implementation of the solar cell model in MATLAB.................................... 11
Figure 2.5: Mono-crystalline solar cell panel (Inc, 2015) 12
Figure 2.6: Shape of Poly-crystalline solar panel.. 13
Figure 2.7: Thin film solar cell (Inc, 2015) 14
Figure 2.8: Silicone diode's characteristic curve (Chaaban, 2011).................................. 15
Figure 2.9: V-I curve for solar cell with neglected Rs, Rsh 15
Figure 2.10: V-I curve and the cell's temperature.. 16
Figure 2.11: Generated Power and voltage in function of variable temperatures 16
Figure 2.12: I-V curve of solar cell under different irradiation values.............................. 17
Figure 2.13: P-V curve in function of the irradiation of the cell, T=25 C......................... 17
Figure 3.1: Different connection configurations of solar cells.. 19
Figure 3.2: Bypass diodes connection in parallel with solar modules............................... 21
Figure 3.3: Generated power and current of partial shaded bypassed system................... 22
Figure 3.4: Irradiance equalization principle... 23
Figure 3.5: 6 by 6 switching matrix structure.. 24
Figure 3.6: Structure of the system after reconfiguration.. 25
Figure 3.7: Flow chart of the reconfiguration process.. 27
Figure 3.8: Adaptive banking method structure 28
Figure 3.9: Structure of adaptive switching matrix 29
Figure 3.10: Flow chart of the first adaptive algorithm.. 29
Figure 3.11: Structure of the adaptive bank before and after reconfiguration................... 31
Figure 4.1: PV panels used in the simulation 35
Figure 4.2 : The performance of the solar system under no partial shading conditions..... 36
Figure 4.3 : Power generation and V-I curve (case2, SP topology) 36
Figure 4.4 : Power generation and V-I curve (case2, TCT topology) 36
Figure 4.5 : Power generation and V-I curve (case2, parallel diode topology)................. 37
Figure 4.6 : Power generation and V-I curve (case3, SP topology). 37
Figure 4.7 : Power generation and V-I curve (case3, TCT topology). 37
Figure 4.8 : Power generation and V-I curve (case 3, parallel diode topology)................ 38

Figure 4.9 : P-V and I-V curve (case 4, TCT). 39
Figure 4.10 : P-V and I-V curve (case 4, SP). 39
Figure 4.11 : P-V and I-V curve (case 4, parallel diodes). 39
Figure 4.12 : Panel matrix order before and after reconfiguration, case 2. 40
Figure 4.13 : Results of the system after reconfiguration, case 2. 40
Figure 4.14 : Panel matrix order before and after reconfiguration, case 3. 41
Figure 4.15 : Results of the system after reconfiguration, case 3. 41
Figure 4.16 : Panel matrix order before and after reconfiguration, case 4. 41
Figure 4.17 : Results of the system after reconfiguration, case 4. 42
Figure 4.18: Simulation model of the adaptive bank. 43
Figure 4.19: Structure of one bloc in the switching matrix. 43
Figure 4.20: P-V and I-V curves without reconfiguration. 44
Figure 4.21: P-V and I-V curves after reconfiguration. 45
Figure 4.22: Power and current curves in the second scheme (without reconfiguration) .. 46
Figure 4.23: Power and Current of second scheme after using reconfiguration 46
Figure 4.24: P-V and I-V curves without reconfiguration. 47
Figure 4.25: P-V and I-V curves after reconfiguration. 47

LIST OF ABBREVIATIONS

A	Ampere
AC	Alternating Current
BL	Bridge Linked
DC	Direct Current
EAR	Electrical Array reconfiguration
G	Irradiation
HC	Honey Comb
I	Current
K	Boltzman’s Constant
K_v	Voltage Coefficient
K_i	Current Coefficient
MPPT	Maximum Power Point Tracking
PV	Photovoltaic
R_{sh}	Shunt Resistance
R_s	Series resistance
SP	Serial parallel
T	Temperature
TCT	Total Cross Tied
V	Voltage
V_{mp}	Maximum Power Voltage
W	watt

CHAPTER 1

INTRODUCTION

1.1 Introduction

Photovoltaic system is an important component to harvest the solar power through clean and efficient methods. The environmental pollution problems related to the excessive use of fossil fuels are continuously growing. These problems are expressed in harmful environment and climate changes. This led the developed countries to emphasize more on the use of green energy to replace the traditional energy production sources. Electrical energy is one of the most distributed types of energy. It is used daily by billions of people. The production of this energy shares in a great part of the environment pollution. These facts led for more researches on the uses of renewable energy sources to replace the traditional methods. Photovoltaic systems are of the most important clean energy sources because the sun is available all the year. It is considered clean because it emits no wastes except in the first stages of production.

After their installation, PV systems generate electricity from the solar irradiation without emitting any greenhouse gases. In their lifetime that extends for more than 25 years PV panels produce clean and safe energy. One of the most important problems while using PV systems is benefitting the maximum of their power. The curve relating voltage and current of solar cell is variable and depends on temperature and solar irradiation. As a result, the power delivered by the power system is a function of these conditions. In order to achieve the maximum of the power of the solar structure, it is important to force it to the point on the V-I curve at which the power is maximal. This process is done in real time and called maximum power point tracking.

Maximum power point tracking (MPPT) methods are special algorithms used to ensure that photovoltaic systems are continuously offering the maximum power output to the user under variable environment conditions like irradiation and temperature. Using such techniques makes the photovoltaic systems able to adapt to the ambient changes and keep delivering the maximum available power. However, MPPT techniques are suitable and efficient in the case where the target solar structure is illuminated equally and constructed from totally similar elements. In the cases where some shade can affect the illumination of some parts of the solar structure, the shaded part will generate less energy (voltage or current) than the other parts.

Partial shading happens when some cells in a photovoltaic array or panel fall in the shadow that prevents it from being well illuminated. This phenomenon can cause important reduction in power generation in parallel with some harmful effects on the shaded parts of the structure. It is generally unavoidable problem especially in small scale urban systems were shadows occur temporarily due to the existence of different types of obstacles. Even in large scale projects under some cloudy weathers it can cause an important power reduction and system defects. Different solutions were proposed to come over the partial shading problem and obtain the maximum possible power from partially shaded solar systems. Some solutions include using bypass elements to separate shaded parts from the system and prevent any damages from being caused to these parts. Other solutions propose different reconfiguration methods to reduce or minimize the effects of shading on the solar systems.

This work will be pointed toward studying the structure of PV system and its different elements. Maximum power point tracking under normal and partial shading conditions will be presented and evaluated. Some different reconfiguration methods will be discussed and evaluated. The results will be presented and discussed.

1.2 Literature Review

Since the invention of photovoltaic systems, the researchers were motivated to invest in the development of systems based on them. The researches were pointed toward the amelioration of efficiency of power converters, the amelioration of the efficiency of the solar cells, creating algorithms to abstract the maximum power of the solar structures, and to find the best configurations for the solar structures. Recently, reconfiguration of solar power array structures to avoid problems related to partial shading of solar systems has become a hot topic in solar renewable energy.

Electrical array reconfiguration EAR algorithm was introduced to improve the energy production of PV systems under partial shading conditions (Guillermo, Francisco, Robert, Manuel, & Alfonso, 2009) and (Velasco, Guinjoan, & Pique, 2008). The EAR algorithm uses a switching matrix between the PV generator and the MPPT controller. The algorithm determines continuously the best configuration of the PV panels; the switching matrix is switched to construct the connections of the best configuration. Best configuration is found by equalizing the irradiation in the series connected elements or strings.

Researchers in (Nguyen & Lehman, An Adaptive Solar Photovoltaic Array Using Model-Based Reconfiguration Algorithm, 2008) and (Lehman & Nguyen, 2008) proposed an adaptive reconfiguration based on the use of two banks of solar PV generators was proposed. In this topology, one of the banks or the main bank is fixed while the other secondary bank is dynamic or reconfigurable. The control scheme reconnects the elements of the adaptive bank in parallel with those of the fixed bank. The algorithm checks in continuous mode that the generated current of each row of the banks is equal to the other rows' current. In case of non equalized current generation, the adaptive bank is reconfigured to ensure the equalization again. Another reconfiguration structure using fixed and adaptive arrays was presented in (Cheng, Pang, Liu, & Xue, 2010). Fuzzy logic based algorithm with practical circuitry was used to determine the best configuration. The idea of using fixed and reconfigurable banks was discussed in many literature studies like (Parlak, 2013). The author proposed a method of detecting the irradiation levels based on short circuit currents measurement. Although this method implies continuous disconnection of the whole system to measure the short circuit current, the author justifies this by the short duration of measurement of few milliseconds.

Comparison between the different configurations of solar panels under partial shading conditions was presented in (Candela, Dio, Sanseverino, & Romano, 2007). Different connection schemes and topologies were studied and their resulting power generation was discussed. The work presented showed that the parallel connection of all solar panels gives the best results in terms of power generation. However, two problems were present in this scheme; the first is the high generated current that implies extra losses in the next stage of conversion, the second drawback resides in the low voltage generation that implies more use of power converters to increase the generated voltage levels. Other topologies like series connection of parallel banks under symmetrical partial shading were discussed. The effect of non symmetrical shading on series connected banks was also discussed in this work. However, no practical solutions -except from future works- were offered for the discussed problems and partial shading effects in this work.

In (El-Dein, Kazerani, & Salama, 2013), the problem of reconfiguration was formulated as a mixed integer quadratic programming problem. The solution of this problem was found using branch and bound algorithm. This algorithm was claimed to be used with either fully reconfigurable or partially (half) reconfigurable arrays. Simulation results were presented showing the effectiveness of the proposed algorithms. Obtained results showed that the fully reconfigurable arrays generate the highest amount of power compared to the half reconfigurable arrays.

Irradiance equalization algorithm with reconfigurable PV array was proposed and studied in (Storey, Wilson, & Bagnall, 2013). The paper showed that the use of this algorithm increases the generated power by 10% over conventional bypassed PV arrays. No comparison with other reconfiguration algorithms was presented.

Tria, Escoto, & Odulio, (2009) has presented a practical work using microcontroller for a reconfigurable PV array of four panels. A fixed load was used such that the power demand is fixed. The algorithm was simple and uses a build up voltage scheme. The algorithm starts bu using one panel and starts to connect other panels in series until the required voltage is acheived. In case of extra power generation, some panels are excluded from the structure to maintain fixed voltage and current. Main drawback of this structure resides in the use of just 4 panels where partial shading conditions cant be tested. Furthermore, some panels can be excluded from the structure under some conditions which causes some power losses.

Patnaik, Sharma, Trimurthulu, Duttagupta, & Agarwal, (2011) has presented practical implementation of reconfiguration algortihm of 4x4 PV cells. The algorithm determines the shaded cells and the shading level of each cell based on thier measured voltage and current. The algorithm arranges the cells to establish mathched series connected cells.

Discussion on the effects of partial shading on the PV systems was presented by (Balato, Costanzo, & Vitelli, 2015). The paper showed how the efficiency and life-time of solar systems can be increased by the use of reconfigurable PV systems. Guerriero, Napoli, d'Alessandro, & Daliento, (2015) has presented special reconfiguration method based on an on-demand bypassing of shaded panels. No special algorithms were presented to ditermine the panels to be bypassed. However, wireless commands are sent to the controller to bypass some panels. Mostly, prior knowledge of the illumination conditions at different day times is required to generate the control of this structure.

As it can be noticed, the literary of the reconfiguration has important contributions and it is seeing continuous development. More and more researches and new algorithms are being produced each new year.

1.3 Scope and Methods

The objective of this study is to discuss some construction of PV systems and power optimization schemes. The discussion includes power cells, modules, converters, and shading problems. Some of the literature proposed reconfiguration methods will be presented and discussed in this work. Comparison of advantages and disadvantages of these methods will be presented and discussed also. Simulation of chosen cases with some reconfiguration algorithms will be carried out and evaluated. Evaluation of the efficiency of the used methods will be performed based on literature and simulation results.

CHAPTER 2

MODELLING OF SOLAR CELL

2.1 Introduction

Photovoltaic or solar cells are built of semiconductor materials; these materials are capable to generate DC electric current if they are subjected to light or irradiation. Solar cells are typically a few centimetres in size. The first solar cell produced in Bell laboratories in 1954 had a 5 percent efficiency (EL-Moghany, 2011). Solar cells are basically semiconductor diodes. When the p-n junctions of these cells are subjected to light they generate current. It is constructed of several types of semiconductor materials using different technologies of manufacturing (Villalva, Gazoli, & Filho, 2009). In the early times after the invention of solar cells, their cost was not an important issue because they were designed for space applications to provide space ships with their required energy. The efficiency of solar cells has dramatically increased since its invention up to day. Nowadays, the market solar cells' efficiency is about 15-19 percent; prices of these types of commercial cells are suitable. Higher efficiency of up to 45% is expected to be achieved in different laboratory researches and under some special conditions. Special construction and arrangements of solar cells ensure high efficiency and ease of use of generated power. The power generated by solar semiconductors depends on different variables among which the intensity of illumination is the most important. Temperature and incidence angle are of the other most important parameters that affect the power generation capability of the solar semiconductor (Liedholm, 2010). These parameters and their effect on the productivity of the solar cells will be discussed briefly in this chapter of the work. Another factor that affects the efficiency of the solar cells is the wavelength of the falling light.

A solar cell is basically has two layers of silicon p-n junction doped with small quantity of atom impurity. The n layer has one more electron in the external layer; and in the p layer it has one electron less. When the two layers are brought together, the electrons travel from the n layer leaving a positively charged layer; the positive wholes leave the p layer toward the n layer creating a negative charged layer. The migration of electrons and wholes creates an electric field like a barrier of further migration. The existence of electric field prevents the flow of electrons in one direction. The flow of electrons is given a path by using external conductors. **Figure 2.1** presents the structure of the solar cell semi conductor material (Morales, 2010).

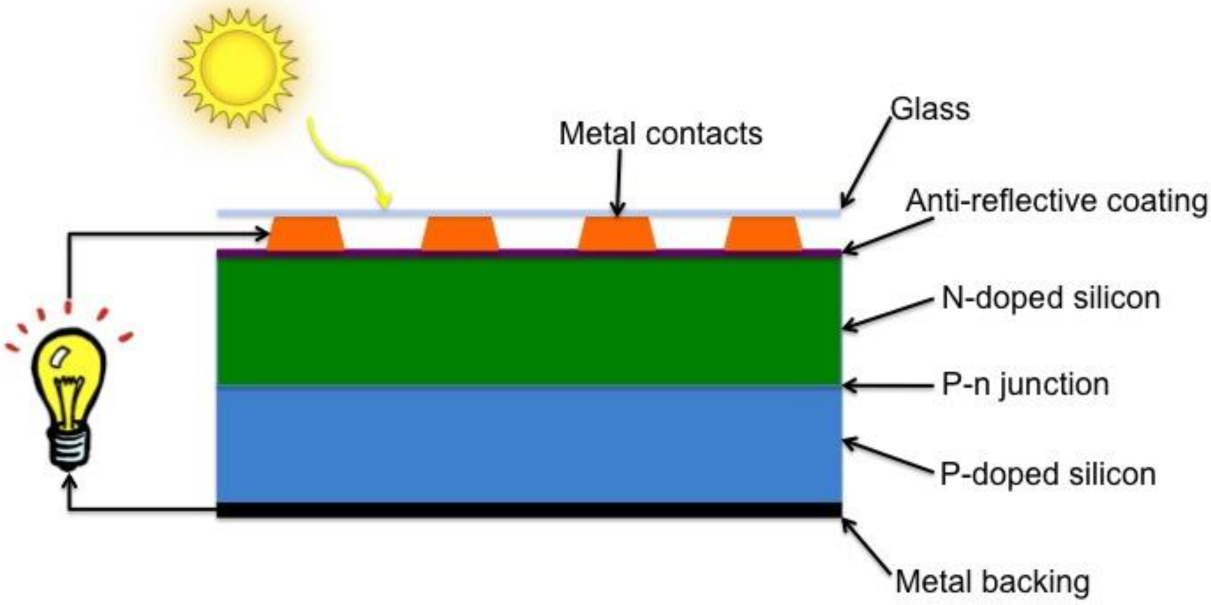

Figure 2.1: Solar cell's structure and components (Barron & Chatelain, 2011).

In order to be able to generate electrical power, electrical voltage and current must be produced. Voltage in the solar cell is generated by a process called photovoltaic effect. Light generated carriers collection by p-n junction causes the flow of electrons from the n type layer and the wholes to the p type layer (Bowden & Honsberg). When the sun light hits the surface of the PV cell, portion of the light's energy is absorbed by the semi-conductor. The absorbed energy increases the kinetic energy of electrons and they start to flow freely. The flow of electrons is described as electrical current generated by the PV cell. **Figure 2.2** presents the working principle of the PV systems. The free electrons flow through the poles of the cells and the external circuit arriving back to the cell after losing their energy. This operation is repeated continuously while there is sun light with enough energy to free electrons (EL-Moghany, 2011).

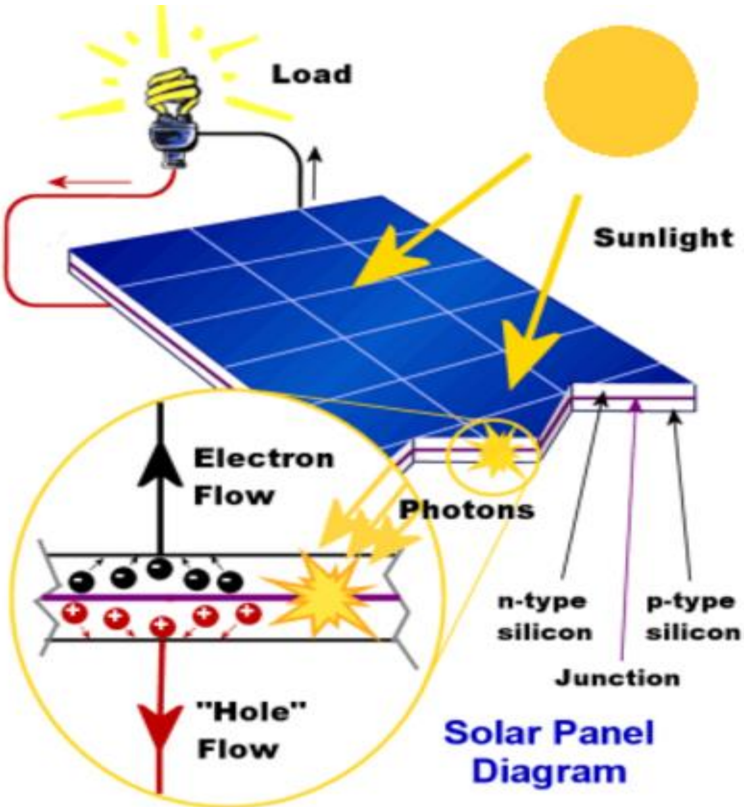

Figure 2.2: Principle of solar cells (Linvents, 2015)

2.2 Equivalent Circuit of Solar Cells

Solar cell models are used to simplify the analysis and simulation of solar systems. The model of the solar cell is a mathematical representation of its equivalent circuit. **Figure 2.3** shows the typical equivalent circuit of a solar cell. This circuit is the simplest model that can describe the function of the solar cell under different conditions. The current-voltage relationship of a solar cell can be defined as follows (Villalva, Gazoli, & Filho, 2009):

$$I = I_{ph} - I_0(\mathrm{e}^{\frac{q(V+IR_s)}{nkT}} - 1) - \frac{V + IR_s}{R_{sh}} \tag{2.1}$$

In this formula V denotes the voltage between the terminls of the diode, I denotes the photovoltaic generated current, I_0 is the dark saturation current; q represents the charge of an electron q=-1.6e-19C. Constant n is a constant describing the diode parameters, k is Boltzmann’s constant and T is the absolute temperature. R_s and R_{sh} represent the series and shunt resistances shown in **Figure 2.3**. In an ideal solar cell, the series resistance would be zero while the shunt resistance is considered infinite to eliminate all electrical losses due to internal resistances and other losses of the cell (Villalva, Gazoli, & Filho, 2009).

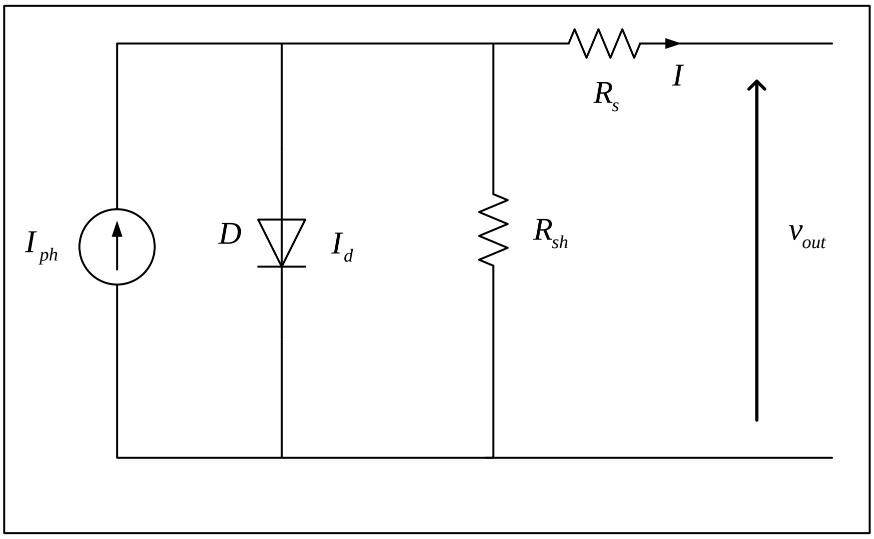

Figure 2.3: Equivalent circuit model of a solar cell

Commercial solar array or module is constructed by combining multiple cells; these cells can be connected either in series or parallel to generate the required level of voltage and current or to fulfil some commercial or technical criteria. In series connected cells, as in any series connection of electrical sources, the generated voltage is equal to the sum of the voltages of the individual cells. The current in this case is equal to that of each one of the individual cells. In parallel structures, the current generated is equal to the sum of the individual currents of the cells while the voltage is the same as that of each one of the cells individually. In the case of multiple cells connected in series or parallel, another term can be added to the last equation to represent the model. An array constructed from N_s cells connected in series. The equation becomes:

$$I = I_{ph} - I_0(\mathrm{e}^{\frac{q(V+IR_s)}{N_s nkT}} - 1) - \frac{V + IR_s}{R_{sh}} \tag{2.2}$$

The photo generated current I_L and saturation current I_0 can be given by the formula:

$$I_{ph} = (I_{ph,n} + K_I \Delta T)\frac{G}{G_n} \tag{2.3}$$

$$I_0 = \frac{I_{sc,n} + k_I \Delta T}{\exp(\frac{v_{oc,n} + k_v \Delta T}{N_s kTn/q}) - 1} \quad (2.4)$$

Where; the small term n refers to the standard conditions under which these values are measured ($1000W/m^2$ and 25° C) (EL-Moghany, 2011) (Villalva, Gazoli, & Ruppert, 2009). The constants k_I and k_v are current and voltage coefficients of temperature. They are related to the structure of the material of solar cell. The term n is the quality factor and k is Boltzmann's number. Based on the previous equations in concordance with the **Figure 2.3** the model of a solar cell can be built using the different given constants. This model can be implemented using SIMULINK/MATLAB to simulate the behaviour of solar cells under different conditions.

The equations describing the system of a solar cell are used to build the system shown in **Figure 2.4**. These modelled equations describe the behaviour of the system under different temperature and irradiation conditions.

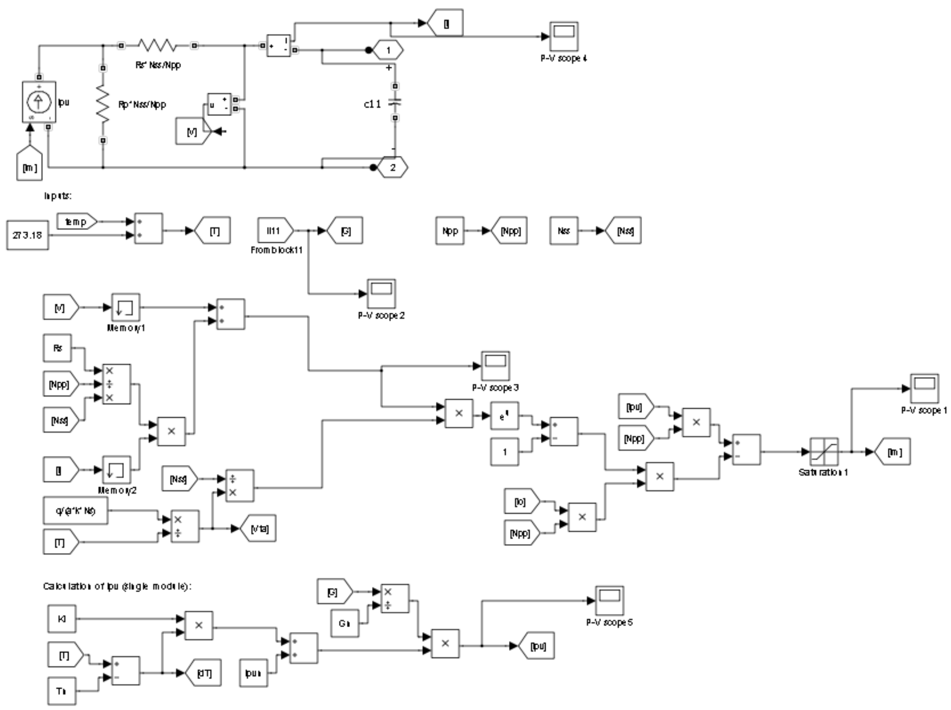

Figure 2.4: Implementation of the solar cell model in MATLAB

2.3 Types of Solar Modules

There exist different types of solar cells in the market of solar energy nowadays. The difference between these materials resides in structural material, price, and light harvesting efficiency. The efficiency of a solar cell is defined as the ratio between the produced electrical energy and the received power from the sun (EL-Moghany, 2011). Unfortunately, the efficiency of the existing solar cells is low relatively. Researchers are intensively working to improve the efficiency of the solar cells as it is one of the most essential parameters of solar energy systems. The maximum efficiency achieved these days doesn't go more than 25%. Mono-crystalline solar cells are considered the highest efficiency type of cells existing in the market today. They are also relatively expensive if compared to other types of cells (Inc, 2015) (EL-Moghany, 2011).

2.3.1 Mono-crystalline cells

Mono-crystalline cells are among the oldest and most efficient solar cells. The module is constructed from a single silicone crystal. They can be recognized by their black or iridescent blue colour. The process of producing mono-crystalline cells is difficult and passes by different stages. The most efficient mono-crystalline cells are produced by SUNPOWER in the United States with efficiency up to 22.5%. Recently, their products efficiency has reached the value of 24.2% (Inc, 2015). **Figure 2.5** shows the shape and colour of a mono-crystalline solar panel.

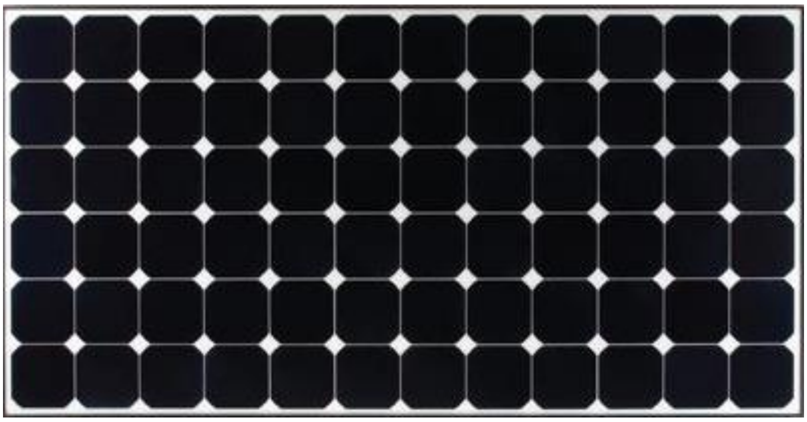

Figure 2.5: Mono-crystalline solar cell panel (Inc, 2015)

Mono-crystalline solar cells proved their ability to work for long time with high efficiency. Some of the modules were installed early in 1970s and they are still producing electricity (Inc, 2015). Although Mono-crystalline panels are more efficient, they suffer from power reduction at higher temperature levels. When the temperature goes around 50 degrees Celsius; the efficiency of the Mono-crystalline cells falls by about 15% (Inc, 2015).

2.3.2 Poly-crystalline cells

This type of cells is constructed from many smaller silicone crystals. They are the cheapest type of solar cells. This is due to the simple fabrication method of poly-crystalline compared to that of Mono-crystalline. They are made by pouring the melt silicone into a cast instead of putting it in one big crystal. The best recorded efficiency of poly-crystalline cells was recorded by Mitsubishi electric and was about 19.3%. This record was achieved by reducing the internal resistance of the module (Inc, 2015). The shape of poly-crystalline cells is like mosaic as shown in **Figure 2.6** (EL-Moghany, 2011).

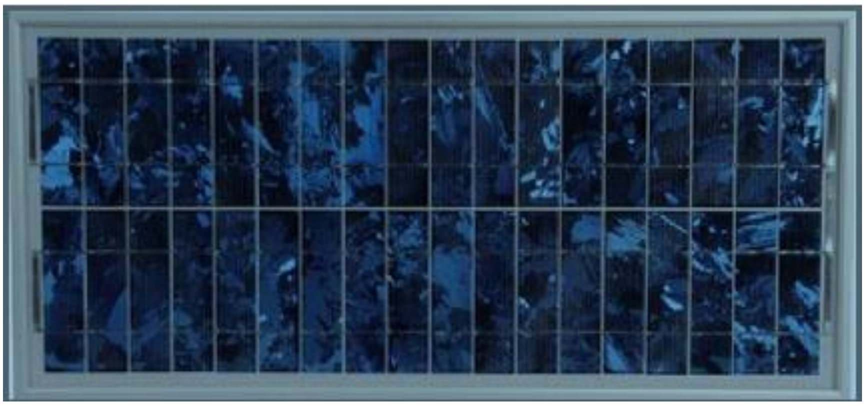

Figure 2.6: Shape of Poly-crystalline solar panel

2.3.3 Thin film solar cells

These solar cells use thin type of photovoltaic materials to produce electricity. Their thickness is about 10 nm compared to 200-300 nm for mono-crystalline and poly-crystalline structures. The junctions in the semi conductors are formed in different way from the other types of solar cells. The aim of producing such thin cells is to reduce the overall production cost per watt of solar energy. The efficiency of this type of panels is about half of that of mono-crystalline. Thin film solar cells are flexible and offer higher performance at indirect light conditions. The efficiency of the thin film modules is higher at higher temperature because they don’t suffer too much from the increase in temperature

(Inc, 2015). **Figure 2.7** presents a small thin film solar cell; it is flexible and very thin compared to the normal mono crystalline or poly crystalline cells.

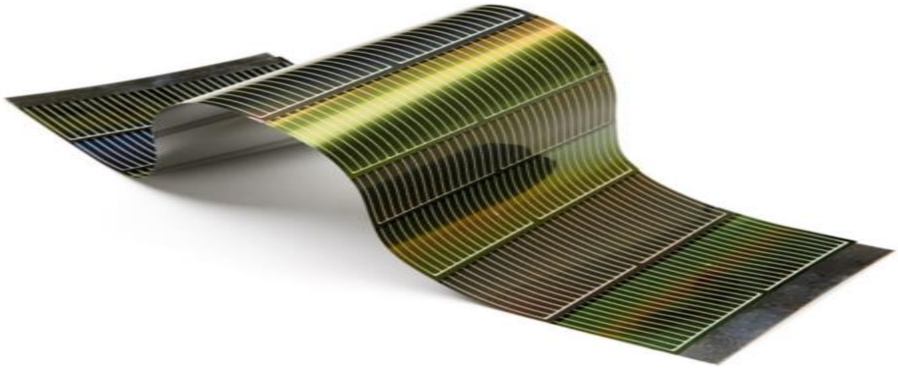

Figure 2.7: Thin film solar cell (Inc, 2015)

Characteristic V-I curve of the PV cell

Characteristics of a solar cell is shown in **Figure 2.8**. The figure is based on the model of the photovoltaic cell shown in **Figure 2.3** and the silicone diode characteristics. In the forward bias zone of the diode, the diode current increases linearly with the voltage between the anode and cathode of the diode. After a specific voltage, the diode voltage starts to saturate and the increase is nearly null. The current of the diode can be given by:

$$I_d = I_0 e^{(\frac{qV}{nkT})} \tag{2.5}$$

where I_0 is the saturation current. The diode's voltage reaches a saturation value where it cannot be increased whatever the value of the forward current.

When the solar cell is not illuminated its behaviour is just like that of the diode. When it is illuminated there exists a fourth quarter as shown in **Figure 2.8**. The characteristic is shifted at the amount of the current generated in the junction of the cell.

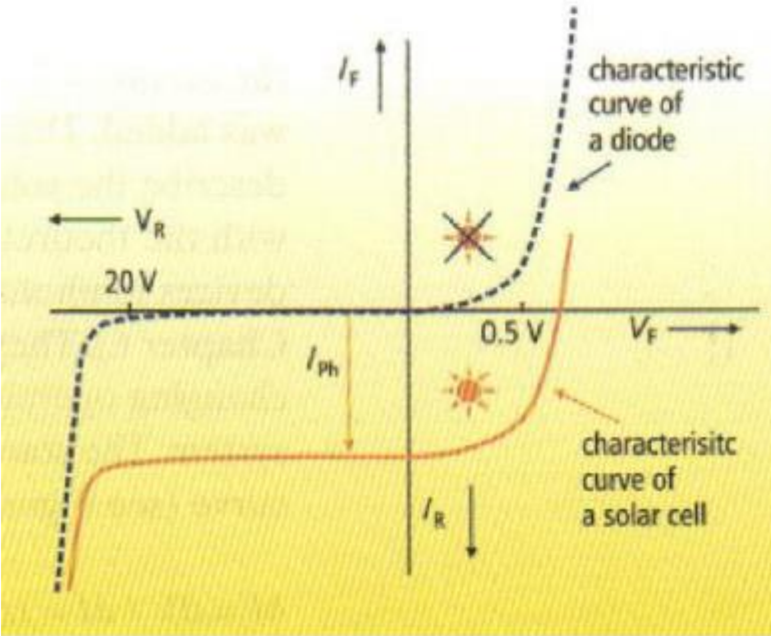

Figure 2.8: Silicone diode's characteristic curve (Chaaban, 2011)

Based on the diode characteristics and considering the equation 2.1 with neglecting the series and shunt resistances the current generated by the solar cell can be calculated. **Figure 2.9** presents the curve of PV cell's current in function of its voltage. The first point of the curve shows the short circuit current while the last point presents the open circuit voltage of the cell. It is important to notice that the open circuit voltage is reduced with the increase of the cell's temperature. The increase of 1 degree Celsius can decrease the voltage by about 3 mV (Bowden & Honsberg). **Figure 2.10** shows the different V-I curves with different temperature values. It shows that the increase in cell's temperature increases slightly the current while decreasing the open circuit voltage.

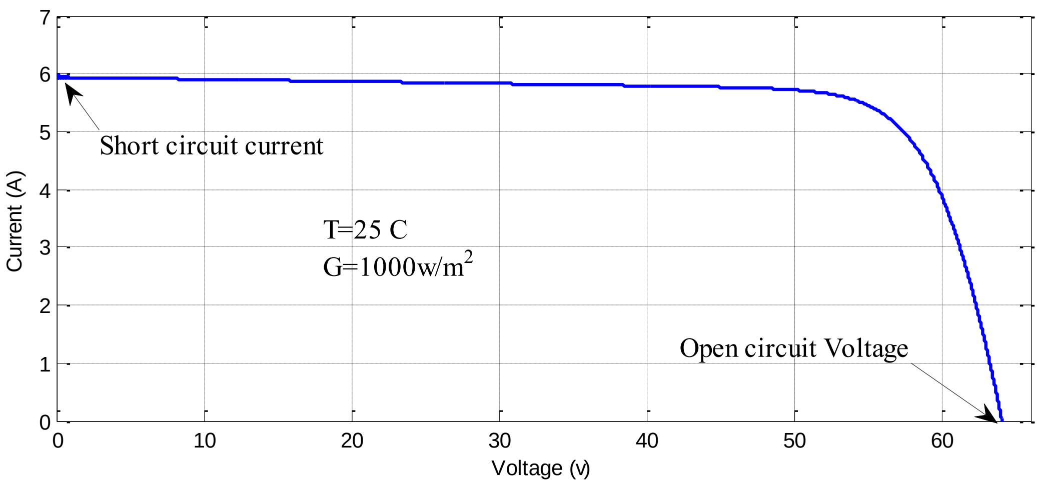

Figure 2.9: V-I curve for solar cell with neglected Rs, Rsh

It is important to mention that all the parameters and characteristics of solar cells and modules are given under Standard test conditions (irradiation of 1000W/m^2, T=298 K).

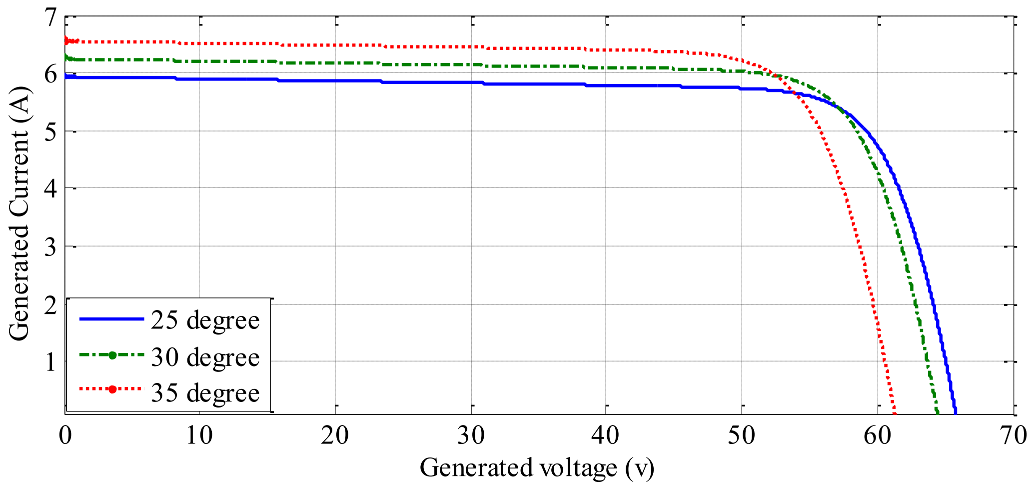

Figure 2.10: V-I curve and the cell's temperature

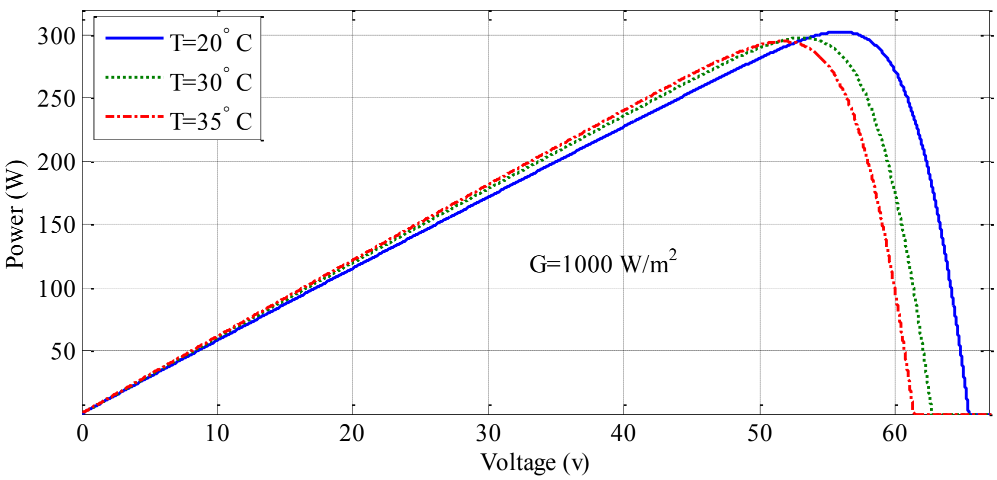

Figure 2.11: Generated Power and voltage in function of variable temperatures

As Figure 2.10 shows, the curve of PV cell is a function of the temperature of the cell itself. The increase in the cells temperature may increase the current generation under constant irradiation, however, the voltage generated by the cell decreases. The curves in **Figure 2.11** present the generated power of the solar cell in function of the cell's temperature. It shows that the increase in the cell's temperature decreases slightly the generated power from the PV cell. Figure 2.12 presents the I-V curve of solar cell under variable solar irradiation. The figure shows that the generated voltage and current decreases when the irradiation decreases. The generated power decreases when the PV cell is subjected to lower irradiation as shown by **Figure 2.13**. The figure shows the power generation at irradiation of 1000, 800, and 500 W/m^2. It's clear that the best power generation is achieved under higher irradiation values.

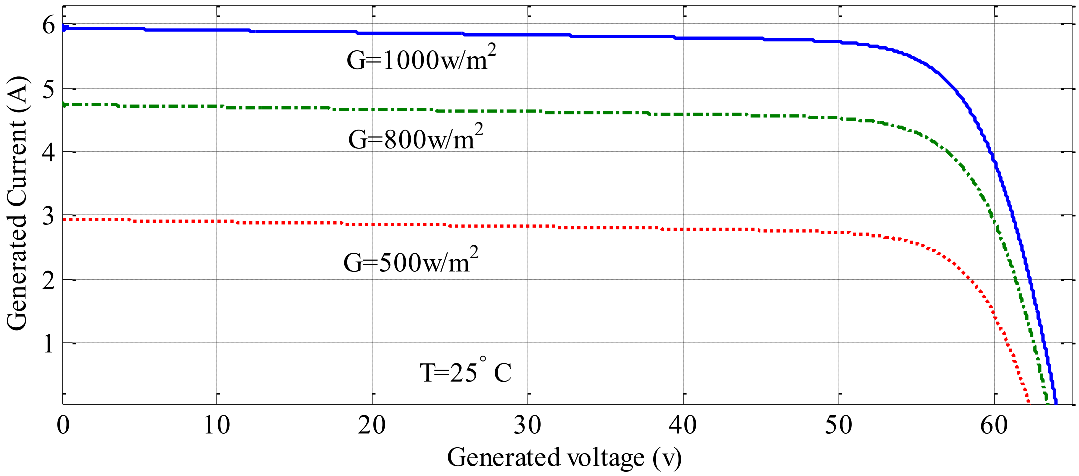

Figure 2.12: I-V curve of solar cell under different irradiation values

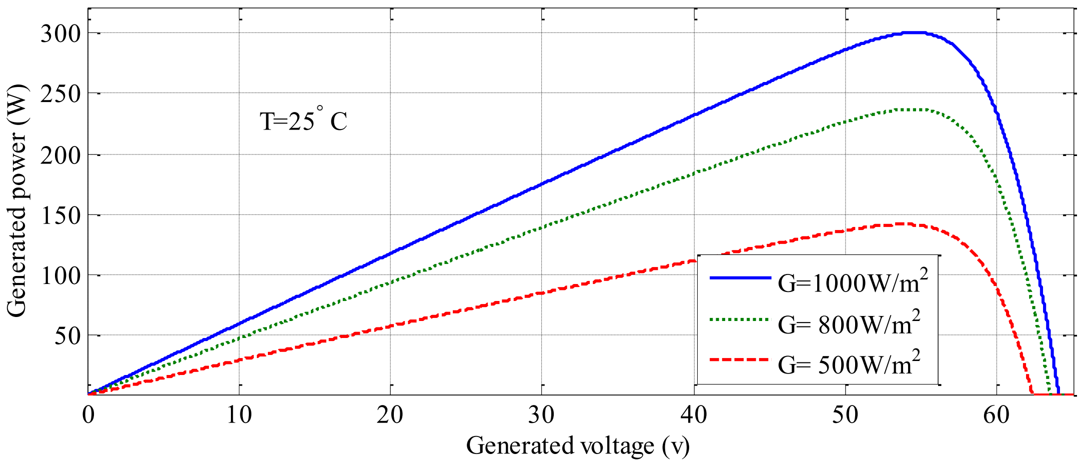

Figure 2.13: P-V curve in function of the irradiation of the cell, T=25 C

CHAPTER 3

RECONFIGURATION OF SOLAR SYSTEMS

A PV array can be created by connecting multiple PV modules in parallel, while a string can be created by series connection of multiple PV modules. In PV systems, one or some of the solar module can be shaded as an effect of clouds, buildings, or trees. The shaded module's power will decrease eventually. If this module is connected in series with other non shaded modules, the current of all series connected modules will be determined by the shaded module. The shaded module or cell will act as a load that absorbs the power generated antecedent or following cells. As an effect, this module's temperature will be increased causing the so called "hot spot" phenomena and destroy the shaded cell (Shaaban, 2011). Shading causes different problems to the PV systems. It reduces the power generated by the solar cell or module, causing mismatch losses in the system. It also creates hotspots that can damage the shaded cell or module and stop its functionality (Shaaban, 2011). Different measures have been studied to overcome the partial shading effects on the PV systems. These measures differ between passive and active methods. Passive methods are easy, inexpensive comparative to the active methods, but they suffer from their low efficiency in terms of power generation. Bypassing diodes can be connected in anti parallel with one cell or string to provide a way for the full current in case of partial shading. Some companies use individual MPPT (in the form of micro inverter) for each one of their panels (Shams El-Dein, 2012). This way each panel is guaranteed to provide its maximum power even under shading conditions (Solar Micro Inverter, Enphase, 2016). This method is a bit costly as it implements a device for each solar panel. Another solution that can be adapted to avoid the partial shading problem is to use adaptively configurable structures that can be changed based on the different conditions. This way the dynamic search for the best connection of PV structure is done in an adaptive way. Many researchers have focused on the configurable PV systems in the last few years in order to increase PV systems efficiency and avoid the risk of destroying shaded parts of it. Reconfiguration is actually suitable to be used for systems at low power range rather than high power applications as the partial shading happens generally in small systems used inside rural or city areas.

3.1 PV Configurations (Interconnection Schemes)

In photovoltaic systems, there are four main configurations that can be used. Each one of these configurations has its own advantages and disadvantages. These schemes are series parallel connection (SP), Total cross tied connection (TCT), bridge linked connection (BL), and Honey Comb connection (HC) as shown in **Figure 3.1** (Shams El-Dein, 2012).

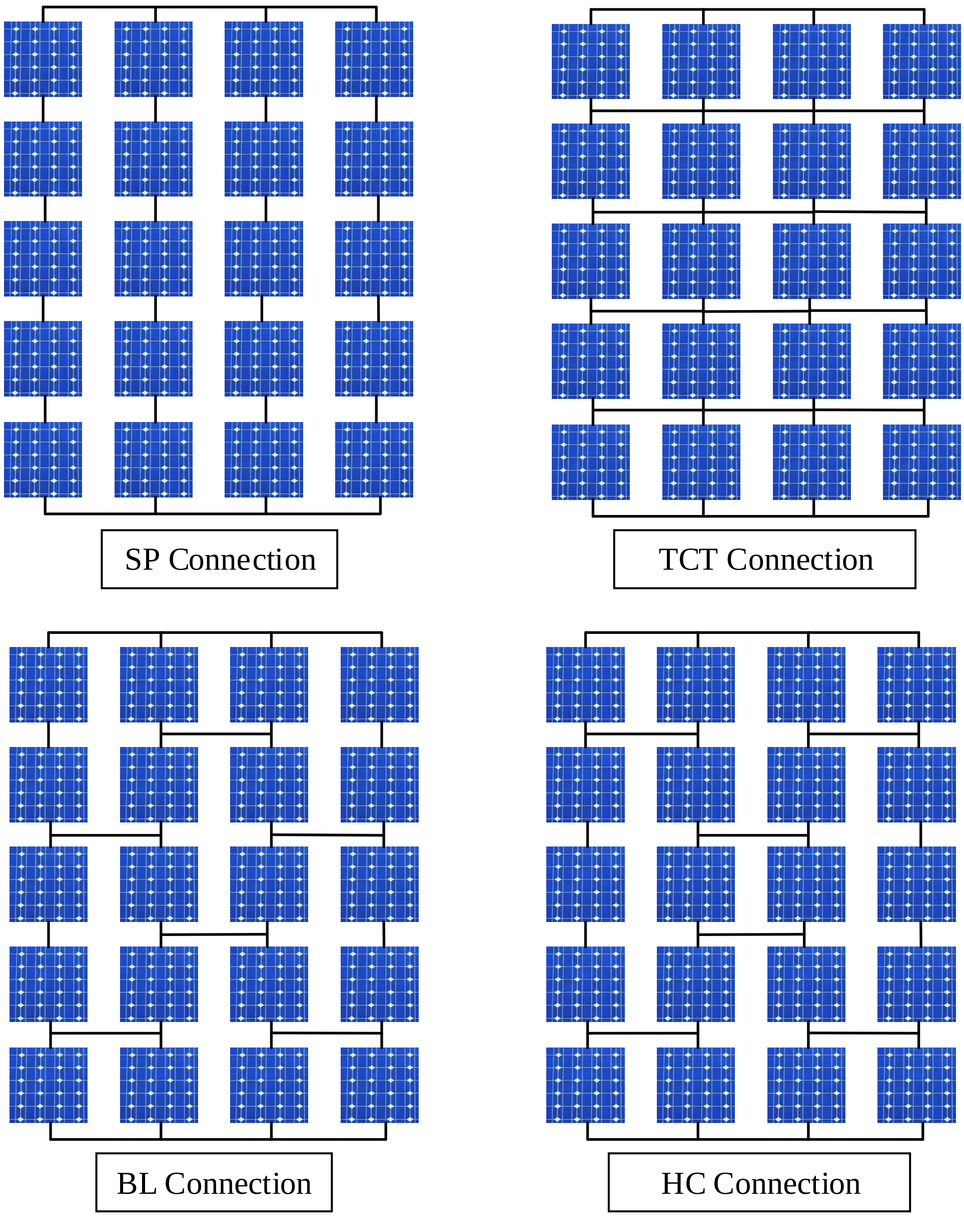

Figure 3.1: Different connection configurations of solar cells

The series parallel connection is the parallel connection of different series connected elements. The number of series elements constructing the strings must be equal to obtain equal voltages of all parallel strings. This connection mode is less suitable for systems that receive partial shading. The shaded elements produce less current than their series non-shaded fellows. The elements that produce less current will be forced to dissipate some energy of the other elements. The total current flow will then be less and reduction in power will occur. In TCT scheme, the connection can be seen as series configuration of parallel connected modules. It has the advantage over the SP scheme in the fact that the shading effect in one element is distributed on all its parallel colleagues. This offers more flexibility and can reduce considerably the partial shading losses. BL and HC are considered as interconnections between the other two schemes (Shams El-Dein, 2012). These two schemes combine advantages from the last two configurations. However, these configurations are still incapable of offering the solution for some partial shading problems especially when more than parallel elements get shaded at the same time.

3.1.1 Bypassing diode as partial shading solution

Bypass diodes are connected in parallel with a solar cell, panel, or module to offer a free bath for the current of other modules in partial shading conditions. **Figure 3.2** shows the connection of bypass diode in the case of two series modules. If one of the two series modules is shaded, its generated current will be reduced. The diode in this case will offer a path to the difference between the string current and the shaded module current (Serna-Garcés, Bastidas-Rodríguez, & Ramos-Paja, 2016). If the diode is not used, the shaded module will be forced to deliver higher current than the generated current and will act as a load. This in terns will dissipate power in form of heat and reduce the power efficiency. Over more, the shaded module will be heated and a hotspot will happen causing the damage of the PV module.

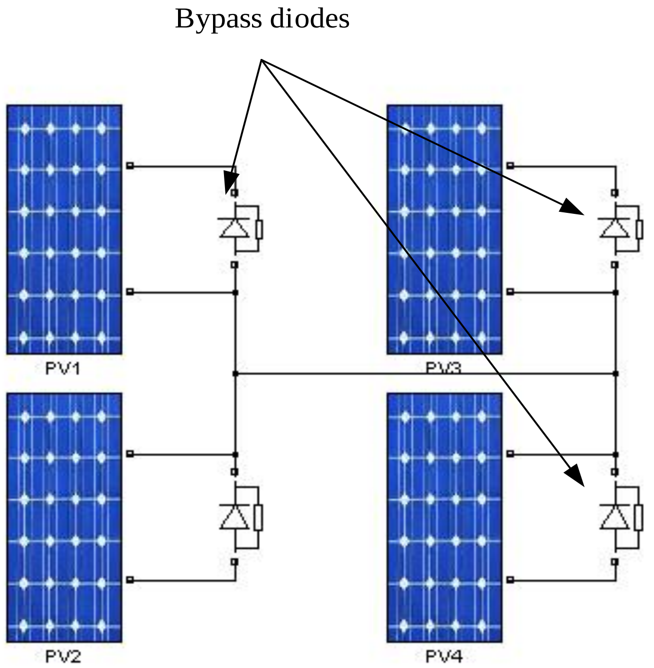

Figure 3.2: Bypass diodes connection in parallel with solar modules

The switching on and off of the bypass diodes implies continuous changes in the P-V curve of the PV system. This curve will have different peaks or maximum power points. The overall characteristics of the grid will change eventually. As the figure shows, the shaded module is producing less current than the normally irradiated modules. As these modules are connected in series, the same current is to flow through the series branches. This implies that the current difference will flow through the diode instead of being forced through the shaded panel. Bypass diodes increase the overall generated power from a PV system under partial shading condition. However, the multiple power peaks created by the bypass diodes affect the function of MPP tracking systems preventing them from finding efficiently the global MPP (Shams El-Dein, 2012).

As mentioned earlier, the use of bypass diodes in parallel with the modules or arrays can prevent the hotspot phenomena. However, it causes the shaded parts to be eliminated from the system whenever the diode conducts. A system composed of 24 PV panels is going to be used to show the effect of bypass diodes under partial shading. The parameters of the used PV panels will be presented within CHAPTER 4. One of the most important drawbacks of the bypass diodes in the case of partial shading is the creation of multiple maximum power points as shown in **Figure 3.3**. The figure presents the generated current and power as a function of the system's voltage. The system is composed of 24 arrays connected in SP structure and bypassed individually by diodes. Out of the 24 arrays, 21 arrays are 100% illuminated with 1000W/m^2. The other three elements are 5% illuminated. The multiple peaks shown in the figure affect the operation of maximum power point tracking algorithms and decrease their efficiency. As it is demonstrated by the figure, the P-V curve has three maximum power points correspondent to the shaded modules.

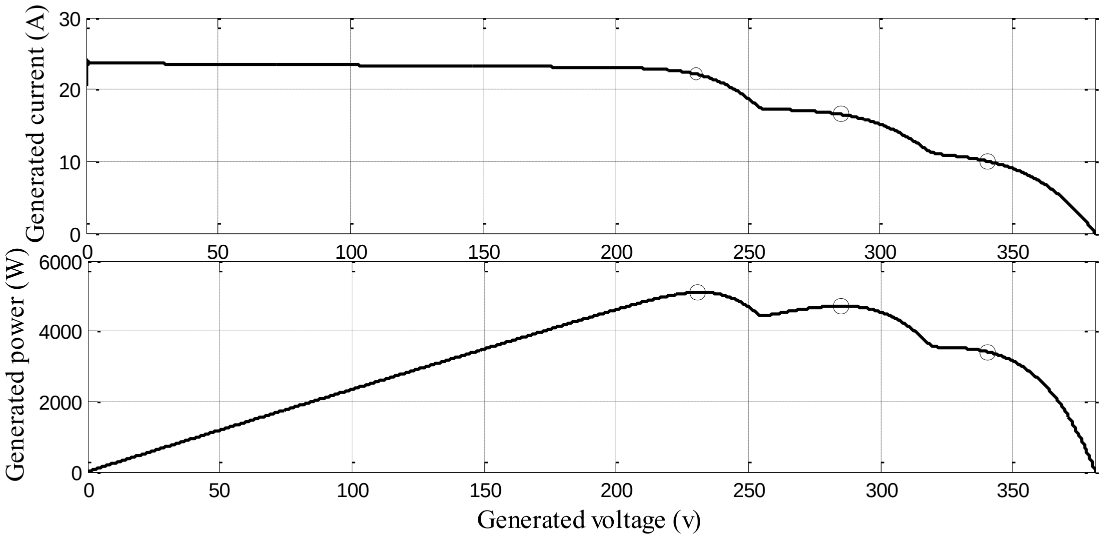

Figure 3.3: Generated power and current of partial shaded bypassed system

3.1.2 Irradiance equalization method

In this method, depending on the illumination received by the modules they are rearranged such that each row of the structure receives the same illumination as the other rows. The rearrangement of the modules or arrays is achieved by implementing switching matrix. **Figure 3.4** explains the idea of irradiance equalization method (Buddha, 2011). Suppose having 9 modules connected in three series arrays. If the illumination of each module is as shown in the **Figure 3.4**-a, the algorithm will try to find another configuration like the one in **Figure 3.4**-b. The idea is to make the total irradiance in the rows equal. This way, the current flows equally from one row to the other. In the case of unequal illumination like b, the current of the lower row (G=1200) is more than the current of the middle row (G=900). The latter produces more current than the upper row (G=600). As a result, the middle row will limit the current of the lower row. Also, the upper row will limit the current of the middle row. The total current will be limited by the least illuminated row (as they are series connected). The less illuminated rows will suffer from heating as higher power is forced through them and they act as loads for the higher illuminated rows. By arranging the modules such that each row produces the same current as the other rows, the hotspot problem can be solved and all the power of the modules can be used effectively.

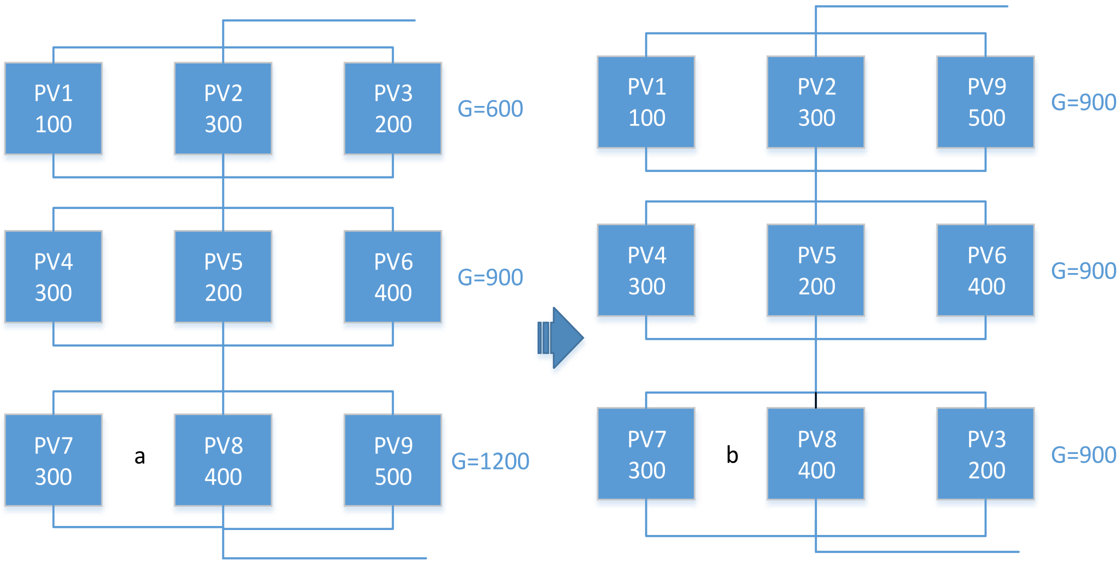

Figure 3.4: Irradiance equalization principle

3.1.3 Dynamic electrical scheme configuration

It is known that the optimal configuration for a set of non-uniformly irradiated PV panels is the parallel connection. However, this configuration is practically impossible because it can't satisfy the maximum current limits of the connected power converter -Inverter or MPPT- (Romano, et al., Optimization of Photovoltaic Energy Production through an Efficient Switching Matrix, 2013). It also can't satisfy the condition of minimum voltage delivered by the system to the power converter. On the other hand, it was noticed that the series connection of non-uniformly irradiated PV modules gives the maximum power out of them (Candela, Dio, Sanseverino, & Romano, 2007). The DES scheme consists of series connection of parallel connected modules "Total Cross Tie TCT".

The proposed reconfiguration system is composed of a control model that implements an optimal reconfiguration algorithm; and a switching matrix responsible for implementation of the electrical scheme generated by the reconfiguration algorithm. The switching matrix is shown in **Figure 3.5** that allows the configuration in a single string of parallel connected modules. The constraint on all series arrays is that they have equal average current or irradiation.

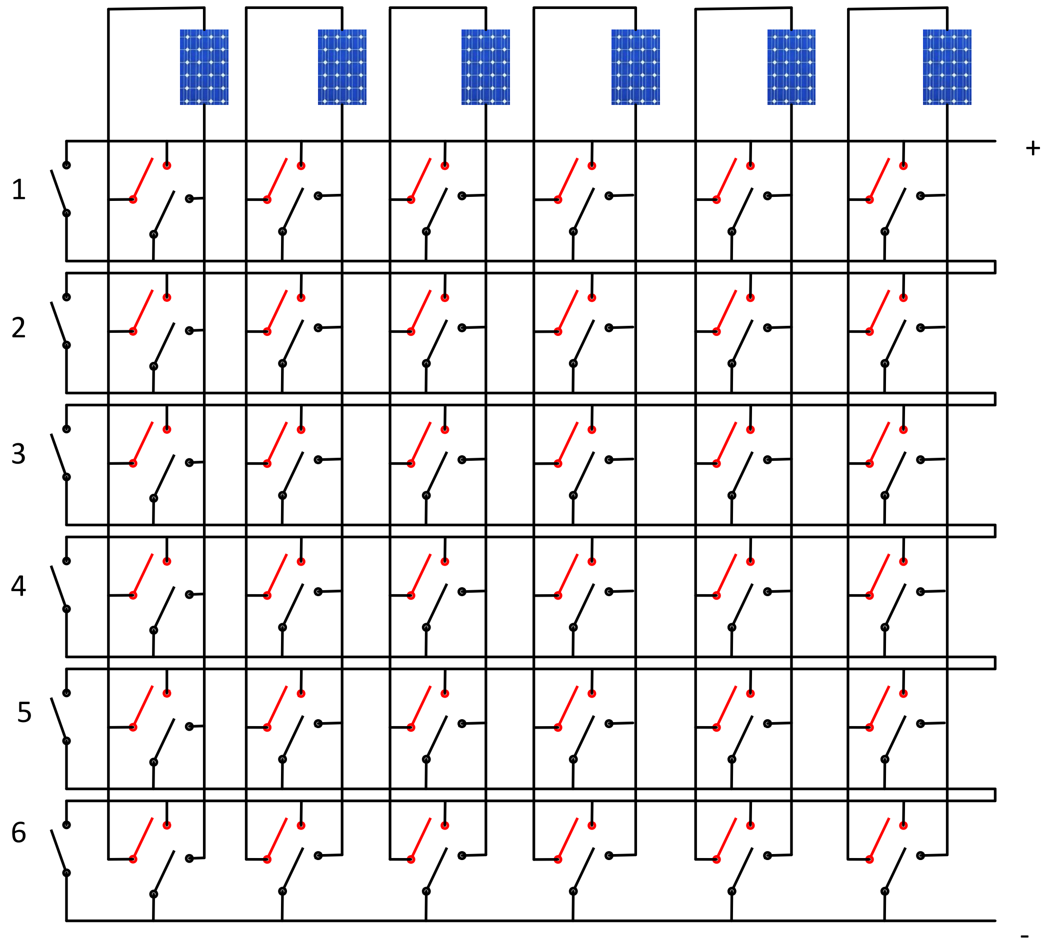

Figure 3.5: 6 by 6 switching matrix structure

It is important to notice that this configuration is totally dynamic in term of the number of series modules and the number of parallel arrays. The limits for the configuration are the maximum allowed voltage and current by the power converter. Hence; the reconfiguration algorithm is in charge of determining the maximum number of parallel arrays and the series modules (Romano, et al., 2013).

The idea is to rearrange the connections of the PV system elements such that the shaded elements don't fall in series connection with non shaded parts. Shaded elements are better distributed in parallel with non shaded elements such that the same current or power is generated by each row of the PV scheme.

The implementation of such a scheme for n PV generators implies the use of n*n double pole switches for the parallel connections. Moreover, other single pole switch is implemented for the series connection of each row of the proposed configuration. That is, the system needs n*{n+1} switches to ensure its function.

The switches used in reconfiguration systems are generally electronic switches (IGBT or MOSFET) or electromagnetic relays that offer low cost and low power losses during the conduction (Balato, Costanzo, & Vitelli, 2015). MOSFET devices are generally low cost devices whose prices are generally less than 2 dollars for general applications. Recalling that the switching of these devices occurs at very low speeds (once each few minutes to reconfigure the system); switching losses of the system are very low.

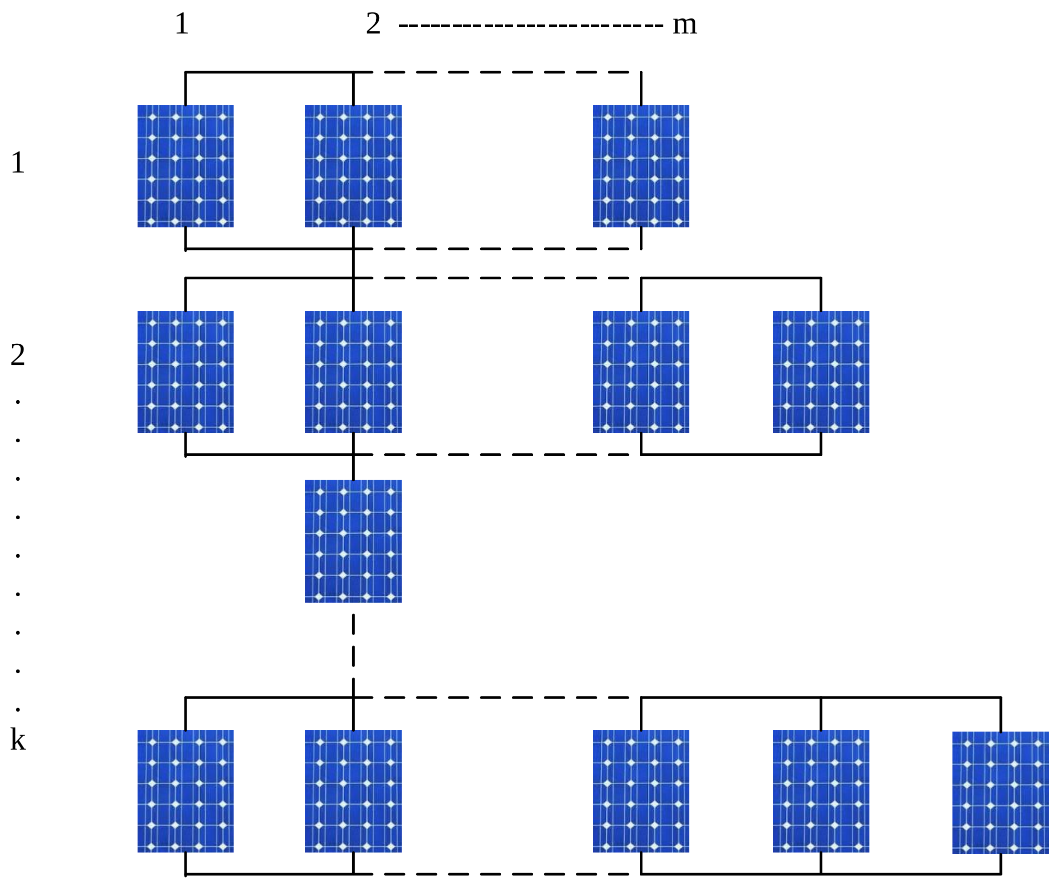

Figure 3.6: Structure of the system after reconfiguration

3.1.3.1 Reconfiguration algorithm

The aim of the reconfiguration is to find the best electrical connection among all possible connections. This connection must ensure the maximum power generation out from the system composed of all solar generators. Mainly, this can be achieved by avoiding the maximum possible the series connection of differently irradiated modules or arrays. The algorithm used implements the irradiance equalization principle. It is easy to implement and allows the power in each row of the series string. This algorithm passes by different steps until the reconfiguration is done. These steps can be resumed as follow:

Step one: Initialization

All system parameters are provided. These parameters include mainly the minimum/maximum number of required rows and the maximum number of parallel modules that can be connected. The minimum number of rows is determined by the minimum and maximum converter voltage on the load side. The maximum number of parallel elements is determined by the maximum current that can be received by the converter or load.

Step two: Data acquisition

The data about the irradiation of each element of the system is measured. This data will be used to find the next connection configuration in the next control loop.

Step three: finding best configuration

The data collected in the second step and the initialization parameters are used to calculate and find the best configuration for the system.

Step four: reconfiguration of the system

The best configuration calculated in step three is now applied to the system. Connections will be changed to fit the new configuration and achieve higher performance of the system (Romano, et al., 2013).

3.1.3.2 Process of finding the best configuration

Finding best configuration is based on a simple search algorithm that employs the acquired (or estimated) irradiation data in its function. This is done by calculation of all possible configurations and finding the optimal one. The total illumination in a row is defined by:

$$G_j = \sum_{i=1}^{n} G_i \tag{3.1}$$

Where n is the number of elements of the row, j is the row number, G is the illumination. For each configuration, an equalization index is calculated by (Romano, et al., 2013):

$$E = \max(G_j) - \min(G_j) \quad , \forall j \tag{3.2}$$

This index shows the distribution of illumination over the rows. Whenever the index is minimal, the illumination is better distributed and all rows have equalized illumination according to (Romano, et al., 2013). The flowchart of the algorithm is shown in **Figure 3.7**. The procedure starts by initializing the parameters, then the illumination values of each module are acquired. These illumination data are arranged from larger to smaller. The configuration then starts by considering the minimum acceptable number of rows and finding the error between the minimum and maximum row illumination. The number of rows is then increased and the procedure is repeated until reaching the maximum number of rows. Upon finishing, the distribution that corresponds to the minimum error is chosen as optimum solution and used to reconfigure the PV system.

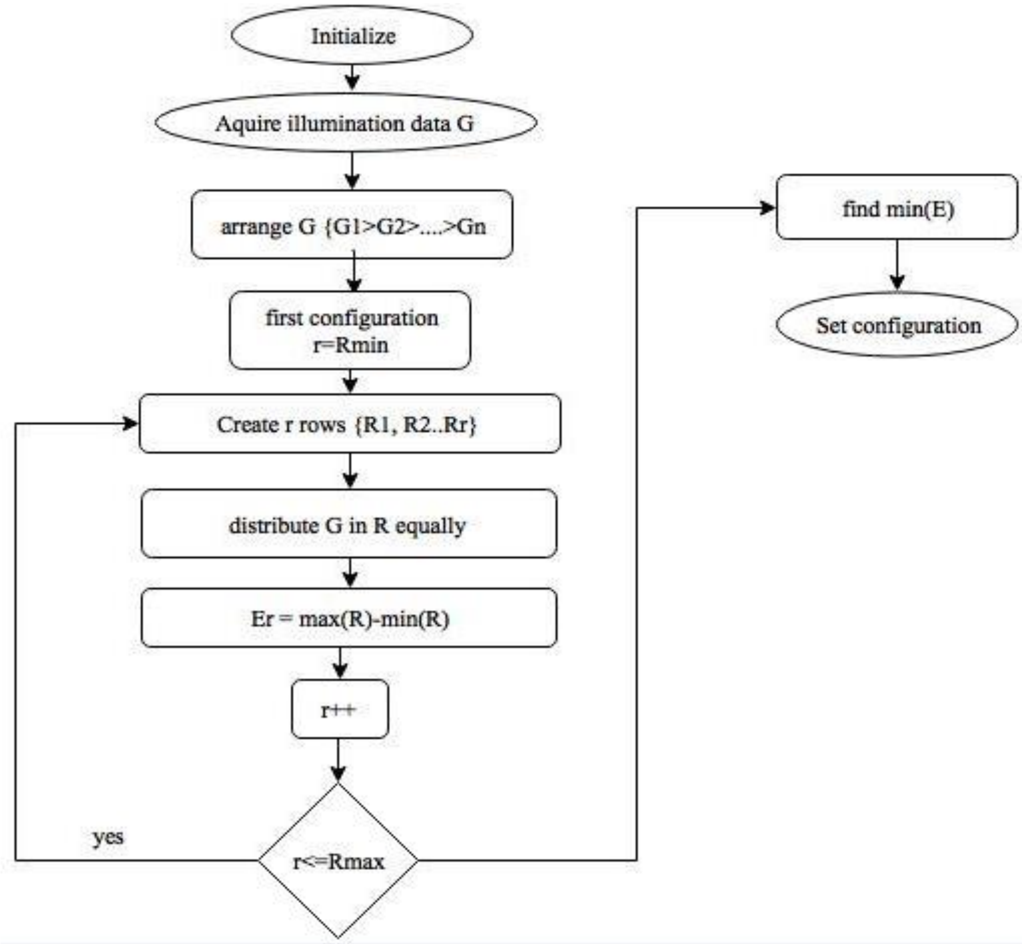

Figure 3.7: Flow chart of the reconfiguration process

3.1.4 Adaptive reconfiguration (adaptive banking) method

This method was presented by (Nguyen & Lehman, 2008) as a practical reconfiguration method. Instead of having all elements of the PV system configurable, it proposes the use of one small reconfigurable bank of PV arrays with larger bank of non reconfigurable arrays. A switching matrix is used to connect the small bank to the large bank. This system reduces the number of used switches and scanning time of algorithm. The arrays connection of the large (fixed) part of the structure is shown in **Figure 3.8**. All fixed part arrays are connected in total cross tied TCT method. It can also be seen as a string of m modules; each module is constructed of n parallel arrays. Connections in this part are fixed and can’t be changed. The reconfigurable part is constructed from m free solar cells that can be individually connected in parallel with any module of the fixed part (Karakose, Baygin, Baygin, Murat, & Akin, 2014) (Velasco, Guinjoan, & Piqué, 2014).

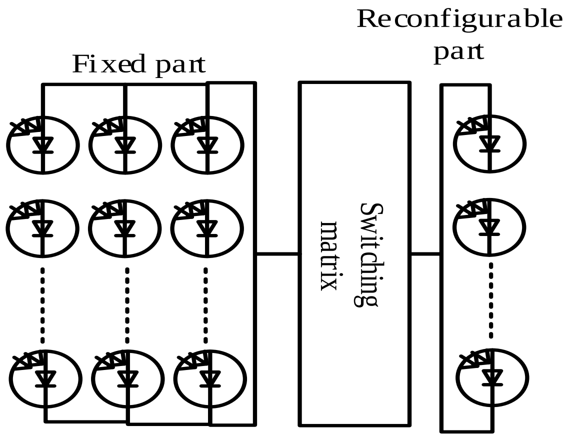

Figure 3.8: Adaptive banking method structure

The switching matrix consists of m by m matrix of switches. Each one of these switches connects one of the adaptive arrays to the correspondent parallel module of the fixed part. Figure 3 shows the switching matrix used in this method. Elements named c_1, c_2, .., and c_m represent the adaptive arrays. Elements R_1,.., R_m are the fixed modules of the system. By activating the switch S(i,j) the array c_j is parallel connected to the module R_i. It is to mention that the switches with the same index j can't be active simultaneously. The activation of each switch of the adaptive bank will be based on the following algorithms.

3.1.4.1 Algorithm 1

The shaded module is detected by comparing its voltage with the average voltage of the other modules. Once a shaded module is detected, one adaptive array will be connected to that module. In the original configuration, the adaptive arrays are arbitrarily connected to the fixed modules. Upon detection of partial shading on one or more modules, the reconfiguration process starts (Nguyen & Lehman, 2008).

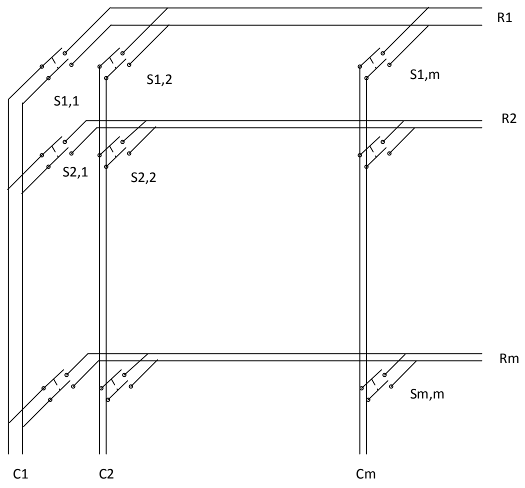

Figure 3.9: Structure of adaptive switching matrix

Reconfiguration process starts by disconnecting all adaptive bank switches, measuring adaptive arrays' voltages, and sorting them in decreasing order such that V1>V2>…>Vm. Voltages of the fixed part modules are also arranged in increasing order from low to high. The switching matrix is activated again such that the highest open circuit voltage of the adaptive bank arrays is connected to the lowest fixed module voltage (the most shaded). And the others are distributed on the same basis. This way the adaptive bank arrays behave like floating balance elements. These elements are continuously rearranged to offer the balance to the system in the case of partial shading. The flow chart of this algorithm is shown in **Figure 3.10**.

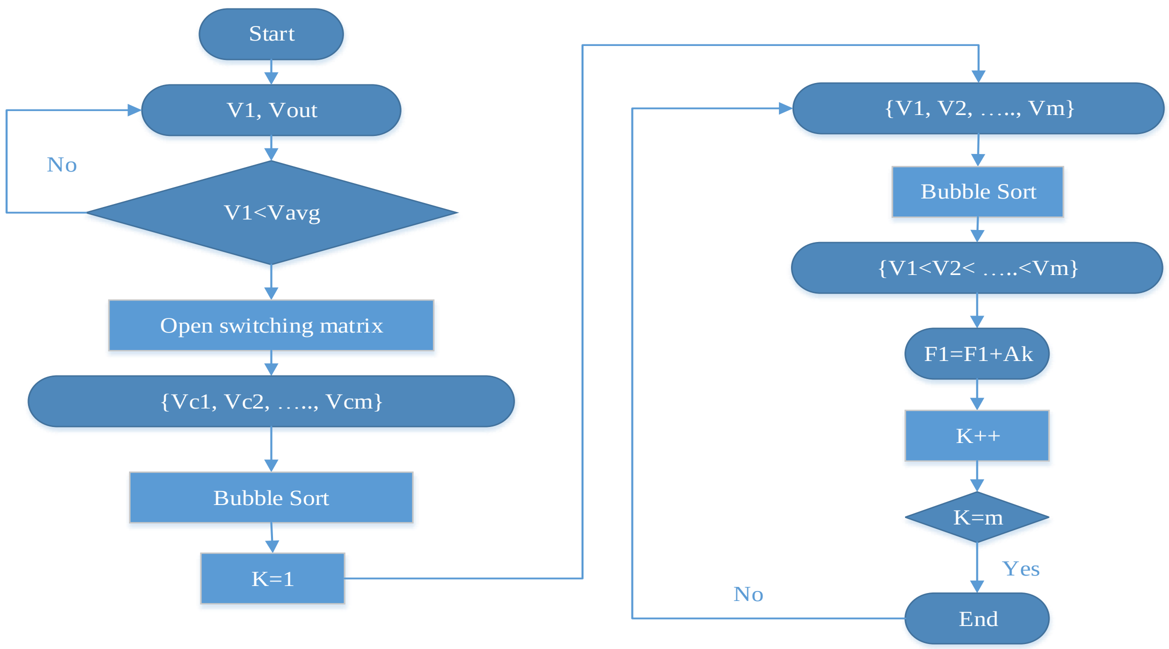

Figure 3.10: Flow chart of the first adaptive algorithm

The bubble sort algorithm is a simple algorithm used to arrange a vector of numbers in ascendant or descendent order. It uses multiple swaps over all the numbers and arranging each pair of numbers. The algorithm stops once the swap does not find any numbers to be arranged.

3.1.4.2 Algorithm 2

In this algorithm, the whole system is connected together and all modules voltages are measured. Adaptive arrays open circuit voltage and temperature of the cells are also measured to be used in the estimation of the arrays currents. The photo generated current of each one of the adaptive bank arrays can be given by (Nguyen & Lehman, 2008):

$$I_{Aj} = \frac{V_{ocAj}}{R_{sh}} + I_s \left[e^{\frac{qV_{ocAj}}{akT}} - 1 \right] \tag{3.3}$$

The currents of the fixed modules can also be estimated based on the equation:

$$I_{Fj} = I_{out} + nI_s \left[e^{\frac{q(V_j + I_{out} R_{sM}}{akT}} - 1 \right] + \left[\frac{V_j + I_{out} R_{sM}}{R_{shM}} \right] \tag{3.4}$$

The estimated currents of the adaptive bank arrays are then arranged in increasing order. Those of the fixed bank are arranged in decreasing order. The least current generating module will be supported by the highest current adaptive array. This way the shaded fixed module will be connected in parallel with the highly illuminated array (arrays) of the adaptive bank as shown in next figure.

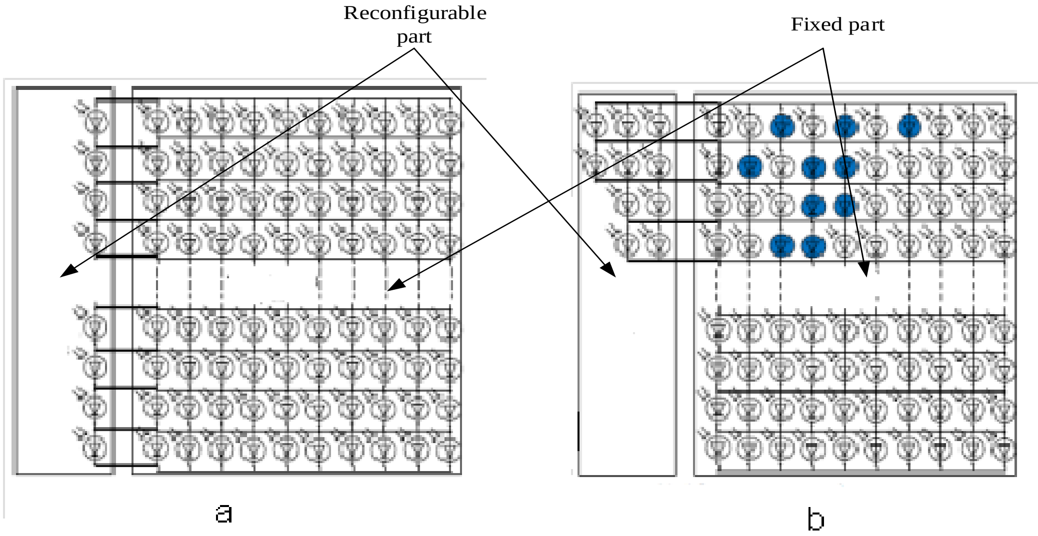

Figure 3.11: Structure of the adaptive bank before and after reconfiguration

3.1.5 Processing Time and Losses of Reconfiguration Process

As discussed earlier in this work, the reconfiguration of the solar systems is meant for decreasing the effect of partial shading of solar systems caused by obstacles like buildings, trees, or any other types of obstacles. Generally, such types of obstacles appear in small power systems in the local and rural areas rather than huge solar plants that are installed outside the residential areas. The dynamic behaviour of the shadow and the movement of the sun are very slow and the shadows occur during long time intervals of few minutes at least. As a result, the changes in the solar configuration are programmed to be either changed at fixed time intervals or upon significant changes in irradiation levels over some parts of the system. The use of NO type relays in the switching matrix was presented in (Cipriani, et al., 2014). Next figure presents a practical switching matrix that is built of Normally Open relays and controlled using a simple ARDUINO microcontroller. In (Karaköse, Murat, Akın, & Parlak, 2014) the authors have presented a study of the processing time of the reconfiguration algorithms where they found that the acquisition and decision time of the different algorithms are generally less than 1.5 seconds.

Switching matrix losses can be considered negligible in solar systems as the switching happens at very low frequency with the changes in the shading parameters over long periods of times. This implied the conclusion that the reconfiguration of solar energy systems is reliable and low cost solution compared with the increase in power generation as will be illustrated in the fourth chapter of this work.

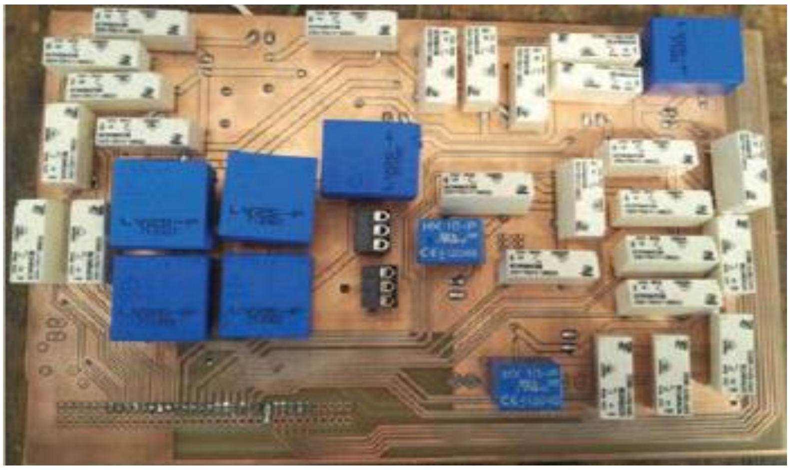

Figure 3.12: Switching matrix of Normally Open relays (Cipriani, et al., 2014).

3.1.6 Reliability of the used reconfiguration system

The reliability of a system is a measure of the ability of the system to function normally before its failure. In solar systems, the balance of system components (inverters, protection circuitries, MPPTs, etc.) represent about 10% of the system cost. However, they are the source of 70% of the solar system failures (Fife, 2010). This is because these components are constructed of large number of electronic and electrical parts whose failure can cause the failure of the whole system. Fortunately, in the solar reconfiguration setup, the system is very simple and needs fewer components like relays or switching devices in addition to the control circuit that includes the software. The circuit components are very simple that can be replaced easily in the case of failure at very low costs. Over more, the control circuit is simple and relies more on the used software.

The switching matrix in a reconfiguration process must provide a strong reliability, low costs, less maintenance, along with high life period like the PV generator itself. In reconfiguration system, different kind of switches can be used like relays, solid-state relays, MOSFETS, IGBTs for their low cost, high performance, high efficiency, high power, and availability. The mostly used switches type is the mechanical relays due to their low prices compared to the solid state relays. In order to decrease the initial costs of using switching matrix, some solutions propose the use of less relays or switches (Manna, Vigni, Sanseverino, Dio, and Romano, 2014). To increase the lifetime of switches, decreasing the number of operations per switch seems to be a good approach. The use of adaptive bank technique presented in this chapter is a good example of reduction of number of switches. The number of operations is reduced mainly by extending the switching time unless it is necessary. That means to make all measurements in continuous mode but make changes on the configuration parameters when these changes are really important to increase significantly the generated power, otherwise, the configuration should be kept unchanged.

CHAPTER 4

RESULTS AND DISCUSSIONS

This chapter discusses the results of reconfiguration using different studied methods in this thesis. The behavior and efficiency of solar systems under partial shadowing will be presented and discussed. Simulation of the proposed reconfiguration method will be carried out using MATLAB/SIMULINK environment. All results will be presented and discussed in the course of this chapter.

4.1 Effect of Partial Shading on the Solar Production

In order to show the effects of partial shading on the different topologies of PV systems the model of the system of the next system was built. The simulation of the system under different conditions was established and results were obtained. Parameters of the simulated system are given in Table 4.1. 24 PV panels will be used in the simulation of the system.

The panels are initially connected as shown in **Figure 4.1**. Different connection topologies were applied on the PV panels. The irradiation levels and shading of the panels for each case are shown in Table 4.2. In the first case, the simulation will consider fully irradiated system with irradiation of 1000w/m^2. The other cases will cover different partial shading conditions. The aim is to test the effect of shading on the different connection topologies of PV systems. Each topology will be tested with all cases.

Table 4.1: Parameters of the PV panels

V_{oc}	64.2 v	$I_{max.\ power}$	5.5 A	k_i	0.0617
I_{sc}	5.87 A	Max. power	300W	k_v	-0.272
Series cells	96	R_p	269.5 Ω	a	0.945
$V_{max.\ power}$	54.7 v	R_{sh}	0.37 Ω	No. panels	24

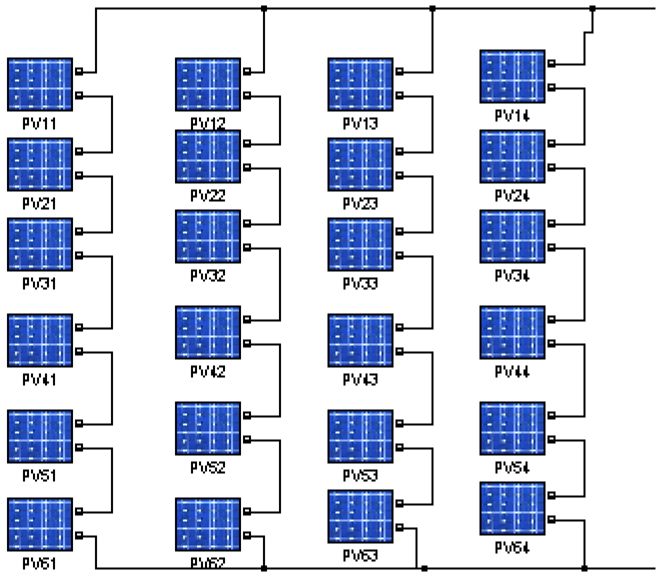

Figure 4.1: PV panels used in the simulation

Table 4.2 : Different shading parameters of the simulated system

Case 1

1000	1000	1000	1000
1000	1000	1000	1000
1000	1000	1000	1000
1000	1000	1000	1000
1000	1000	1000	1000
1000	1000	1000	1000

Case 2

500	1000	1000	1000
500	1000	1000	1000
500	1000	1000	1000
500	1000	1000	1000
500	1000	1000	1000
500	1000	1000	1000

Case 3

500	500	500	500
1000	1000	1000	1000
1000	1000	1000	1000
1000	1000	1000	1000
1000	1000	1000	1000
1000	1000	1000	1000

Case 4

1000	1000	1000	1000
1000	1000	1000	1000
500	1000	1000	1000
500	500	1000	1000
500	500	500	1000
500	500	500	500

4.1.1 Equally distributed irradiation, case 1

In this experiment, the whole matrix of PV panels will receive the same irradiation levels. All the topologies have given the same results with the system at its maximum efficiency as shown in Figure 4.2. The maximum power value was approximately 7.2kW.

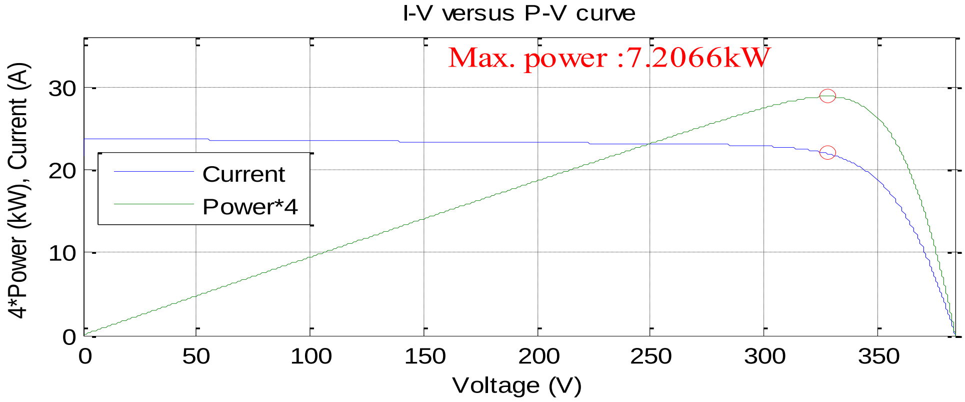

Figure 4.2 : The performance of the solar system under no partial shading conditions

4.1.2 Partial shading of one column of the matrix, case 2

In this experiment, a full column of the matrix was shaded while the other columns were normally irradiated. The results are presented in figures 4.3, 4.4, and 4.5. These figures show that the shading of one column (of series elements) will reduce the generated power for all topologies. It is to mention that the shading was identical for all the elements of the column. 6 series elements were half irradiated which implies a reduction of approximately 900W in the generated power. The generated power has reduced from 7206W to 6254W for all topologies. This means that the partial shading of one column has no effects on the non shaded elements.

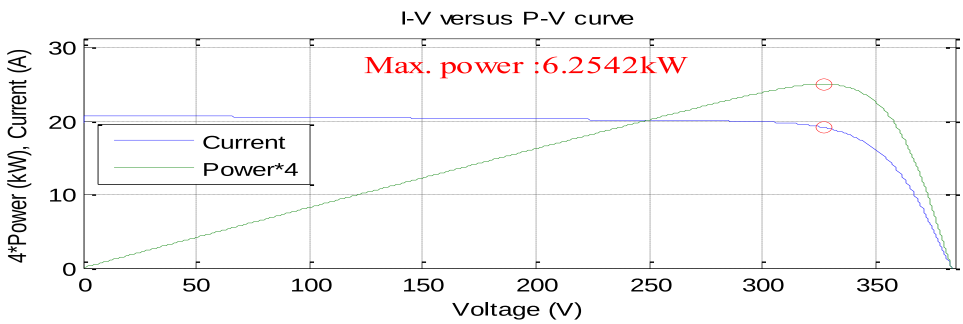

Figure 4.3 : Power generation and V-I curve (case2, SP topology)

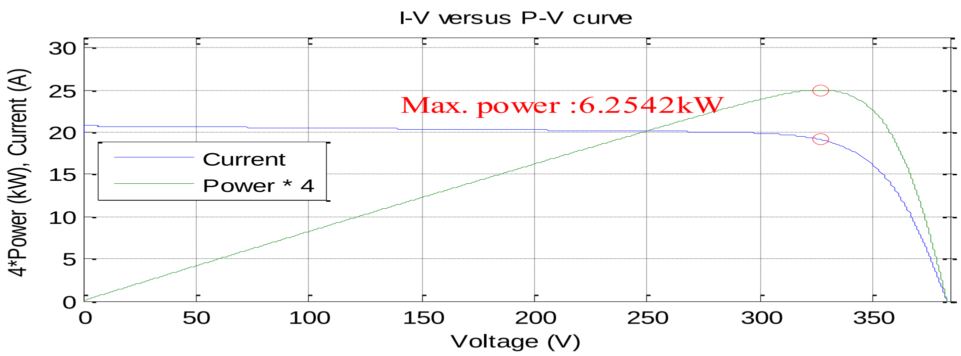

Figure 4.4 : Power generation and V-I curve (case2, TCT topology)

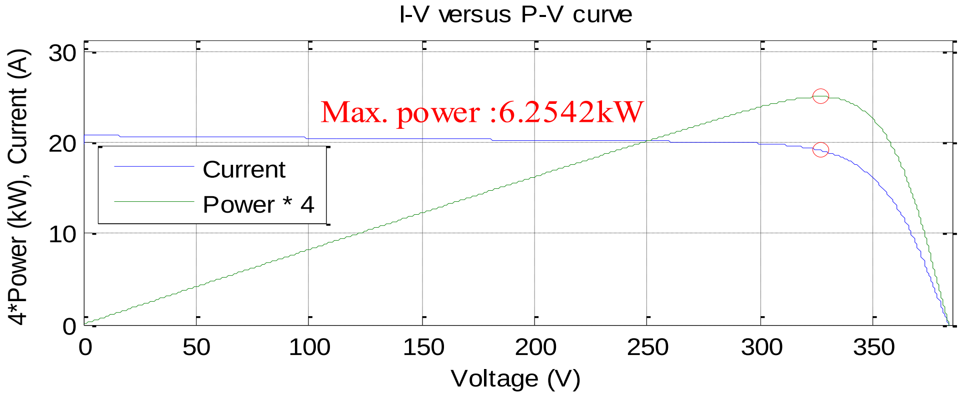

Figure 4.5 : Power generation and V-I curve (case2, parallel diode topology)

4.1.3 Partial shading of horizontal line of the PV matrix, case 3

In this experiment, partial shade was applied on one horizontal line of the PV matrix. The shaded line was illuminated with 500W/m^2. Figure 4.6 shows the P-V and I-V curve of the system connected in SP topology. Figure 4.7 shows these results using TCT topology. These two figures show that the illumination of one line has reduced the power to half the full power. While the real reduction in power should be 600W; the shaded elements were series connected and approximately 3kW were dissipated in the shaded panels.

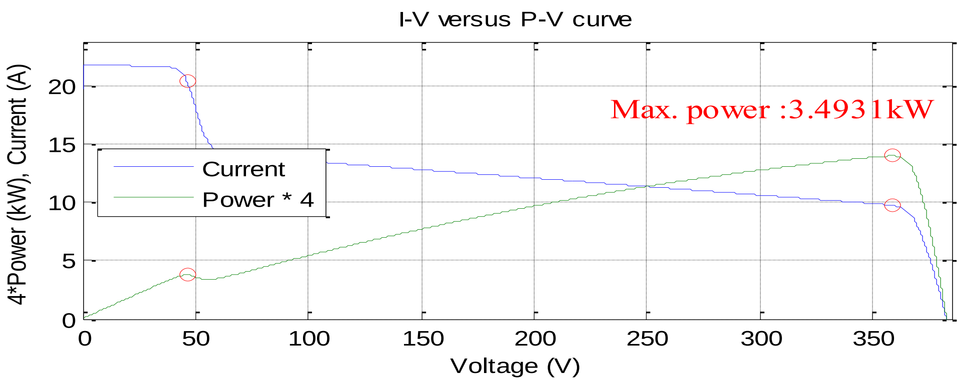

Figure 4.6 : Power generation and V-I curve (case3, SP topology).

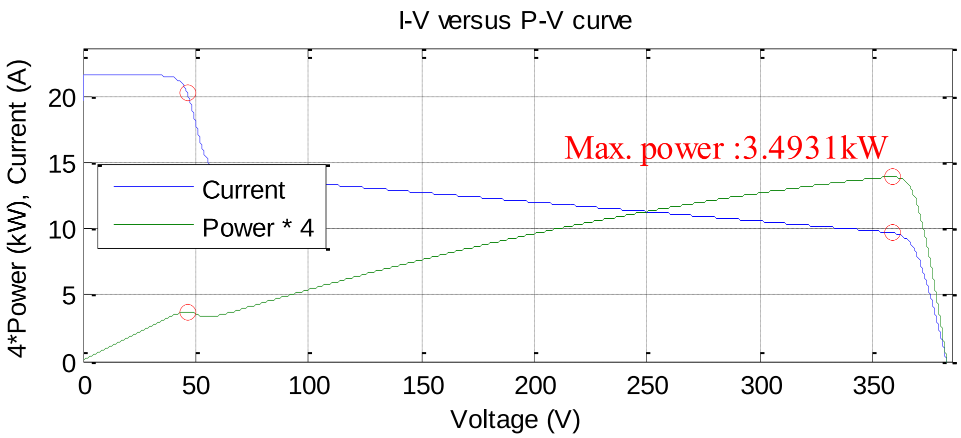

Figure 4.7 : Power generation and V-I curve (case3, TCT topology)

Figure 4.8 presents the use of parallel diode to avoid the effects of partial shading of series connected PV generators. The diode offers a free path for the current generated by series non-shaded PV sources. However, parallel diodes eliminate the shaded PV generator while allow full power generation of the non-shaded elements. Generated power has reduced from 7200W to 5975W as all shaded elements were cancelled and some power dissipation happens due to the use of diodes. 1225W were lost from the system as an effect instead of 600W.

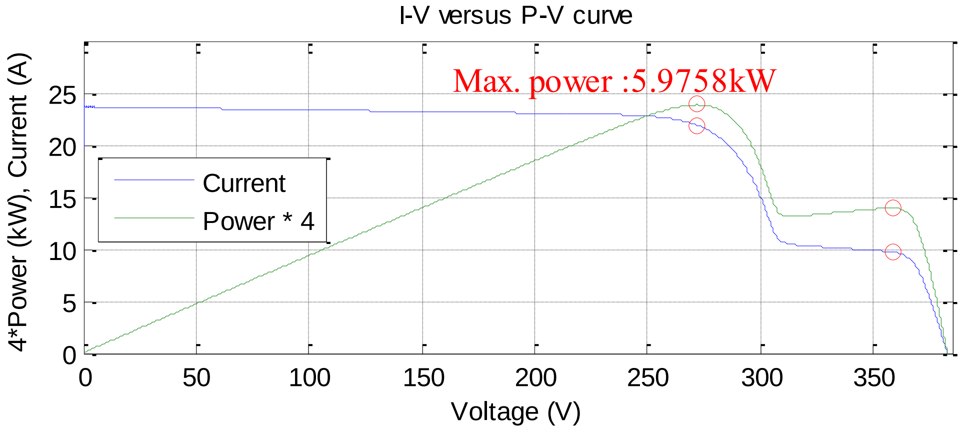

Figure 4.8 : Power generation and V-I curve (case 3, parallel diode topology)

4.1.4 Partial shading of triangular group of elements, case 4

In this case, triangular group of elements containing 10 elements was shaded. This group was subjected to irradiation of 500W/m^2. Reduction of 1500W in the individual generated power was expected. However, simulation results show that the reduction in the generated power is higher. Figure 9, 10, and 11 show that the generated power was approximately half of the nominal power. SP topology has shown the worst results with power dissipation of 3750W. In this topology, the columns containing shaded elements generate power as if the whole column was shaded. The TCT topology has given a little better result as shown in Figure 4.9. However, the power losses are still high. Parallel diodes topology has given the best performance with approximately 3790W. This topology offers the advantage of protection of non-shaded elements from being destroyed due to hotspot effect.

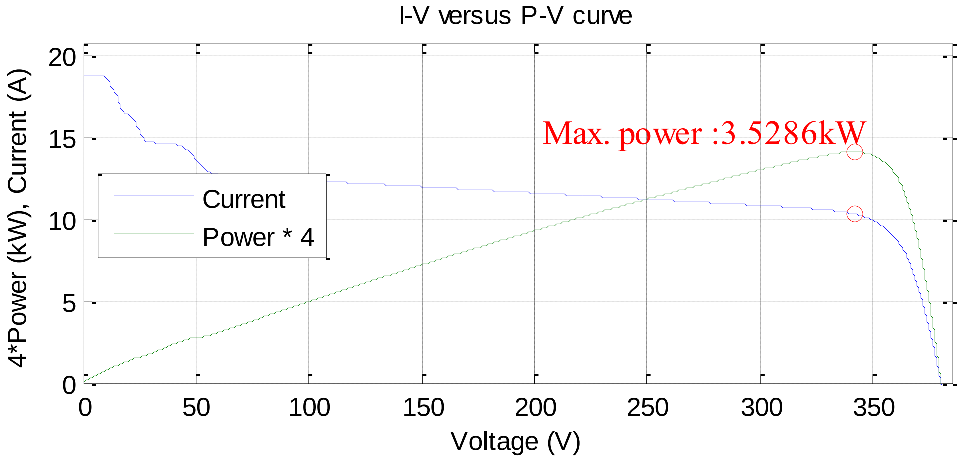

Figure 4.9 : P-V and I-V curve (case 4, TCT).

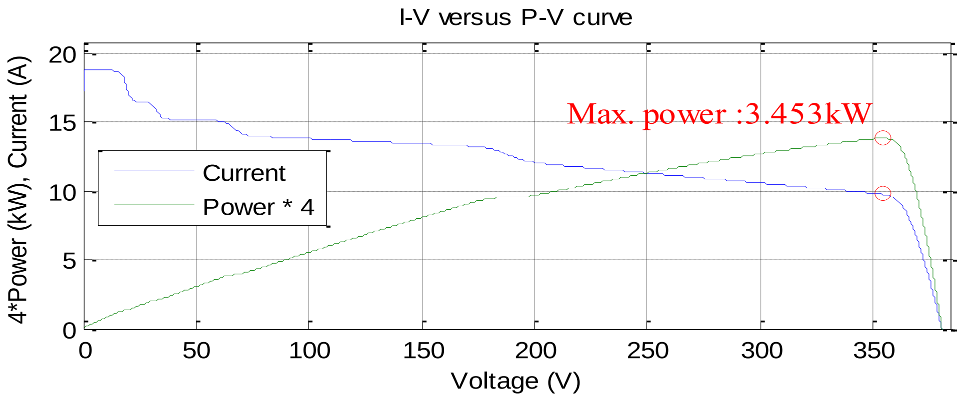

Figure 4.10 : P-V and I-V curve (case 4, SP)

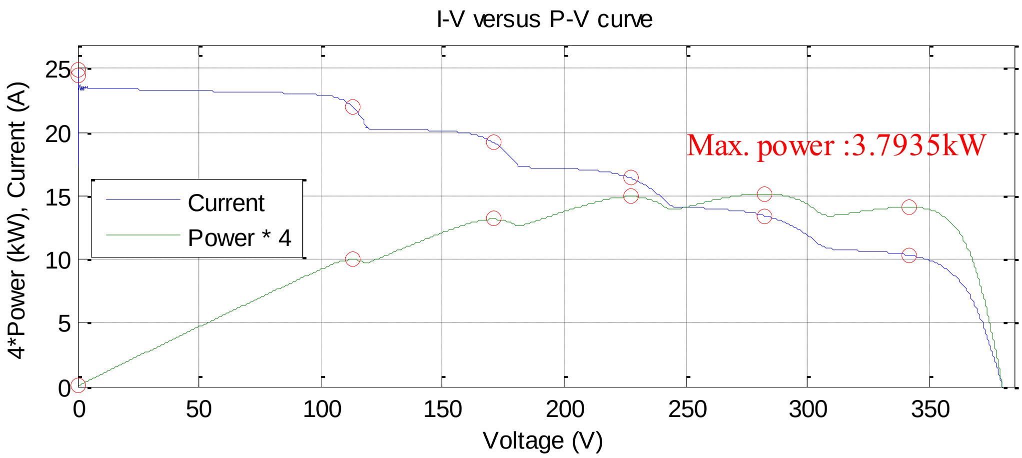

Figure 4.11 : P-V and I-V curve (case 4, parallel diodes)

4.2 Reconfiguration of PV Matrix

In this part, the studied reconfiguration algorithm will be applied on the different cases shown above and other cases. Minimum series connected elements was defined to be 4 (related to the minimum voltage of the system). Initially, the simulation starts with the connection shown in **Figure 4.1**. 6 elements are series connected in each column of the matrix. The algorithm reads the data provided about the irradiation of each element and decide the best configuration topology. Control of the switches is then generated to establish the new configuration ensuring best power generation. The above studied cases 2, 3 and 4 are going to be examined using this algorithm. Full column shading, full line shading, and triangle shading results are shown in the next figures.

4.2.1 Partial shading of one column of the matrix, case 2

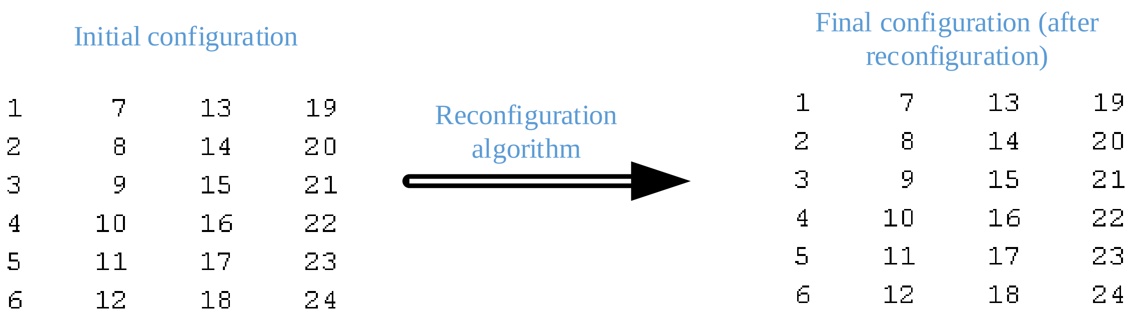

Figure 4.12 : Panel matrix order before and after reconfiguration, case 2

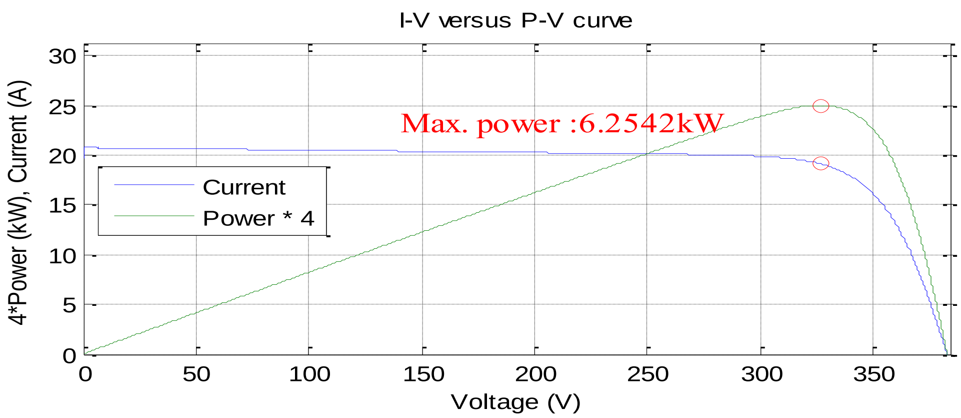

Figure 4.13 : Results of the system after reconfiguration, case 2

4.2.2 Partial shading of horizontal line of the PV matrix, case 3

Initial configuration

1	7	13	19
2	8	14	20
3	9	15	21
4	10	16	22
5	11	17	23
6	12	18	24

Reconfiguration algorithm $\longrightarrow$

Final configuration (after reconfiguration)

1	9	13	17	21	5
2	10	14	18	22	6
3	11	15	19	23	7
4	12	16	20	24	8

Figure 4.14 : Panel matrix order before and after reconfiguration, case 3

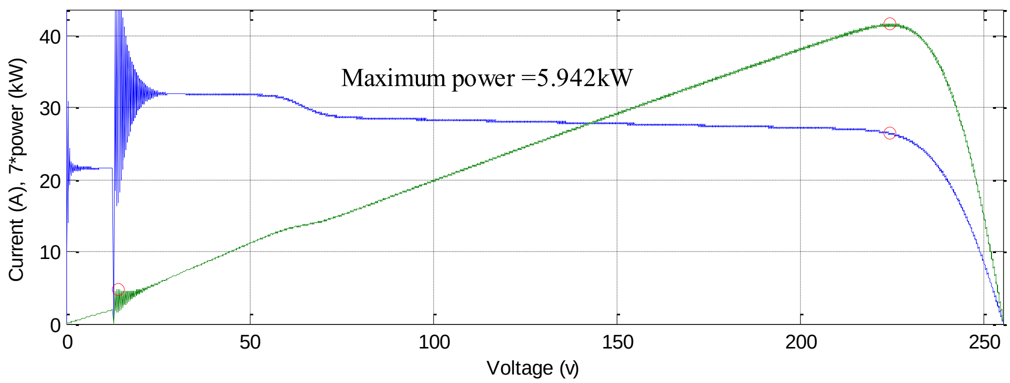

Figure 4.15 : Results of the system after reconfiguration, case 3

4.2.3 Partial shading of triangular group of elements, case 4

Initial configuration

1	7	13	19
2	8	14	20
3	9	15	21
4	10	16	22
5	11	17	23
6	12	18	24

Reconfiguration algorithm $\longrightarrow$

Final configuration (after reconfiguration)

1	12	0
2	15	0
3	16	0
4	20	0
5	9	21
6	13	22
7	17	23
8	18	24
10	19	0
11	14	0

Figure 4.16 : Panel matrix order before and after reconfiguration, case 4

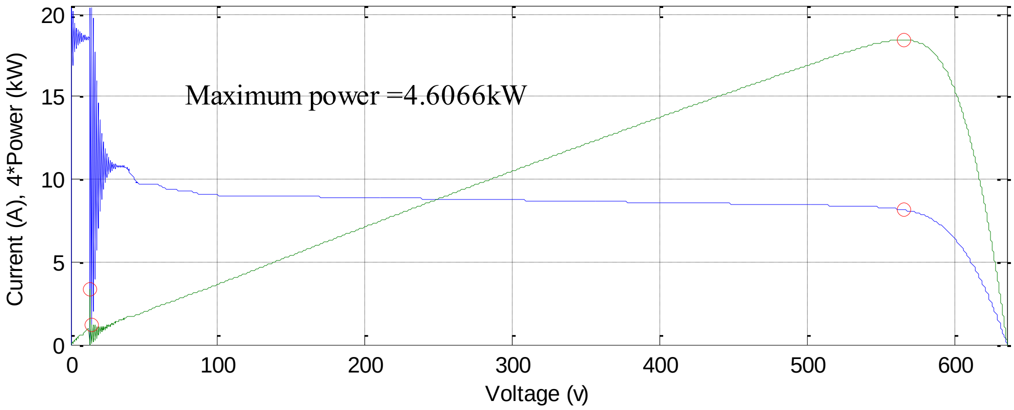

Figure 4.17 : Results of the system after reconfiguration, case 4

As figures 4.12-4.17 show, the reconfiguration process rearranges the connections between the elements of the matrix. The elements of each row in the reconfigured matrix are connected in parallel. The rows are connected in series to establish the total connection of the system. It is clear that the reconfiguration gives the maximum possible power by creating approximately equal current rows at each moment. This way, the configuration implies no hotspot or power losses between mismatched series elements. The transient currents that can be noticed at the switching time are due to the change in the voltage and current of the system. These currents are limited by the short circuit current of the PV modules and their effect can be neglected as the switching occurs at long interval of times (few minutes generally) that depends on the changes in the shading distribution over the time.

4.3 Adaptive Bank Reconfiguration

In this part, the results of the program using adaptive bank reconfiguration are discussed and presented. One column out of our 6*4 solar array elements was used as an adaptive bank while the other 3 columns were considered as fixed bank. Figure 4.18 shows the SIMULINK model of the adaptive bank. The figure shows the switching matrix that is used to switch the connection of the adaptive bank elements to the fixed bank elements. The switching matrix consists of 36 switches that control the connection of the adaptive bank elements with the fixed elements. Each one of the six adaptive panels can be connected to one row of the fixed panels at a time through one switch. Switching matrix contains six different blocs; each bloc is constructed of six double pole switches. The structure of the bloc is presented in **Figure 4.19** where each bloc is able to connect one fixed row to any one of the six adaptive elements. The adaptive element can be connected to one row at the moment and careful must be taken to avoid the connection of the same adaptive element to more than one row as it causes short circuit.

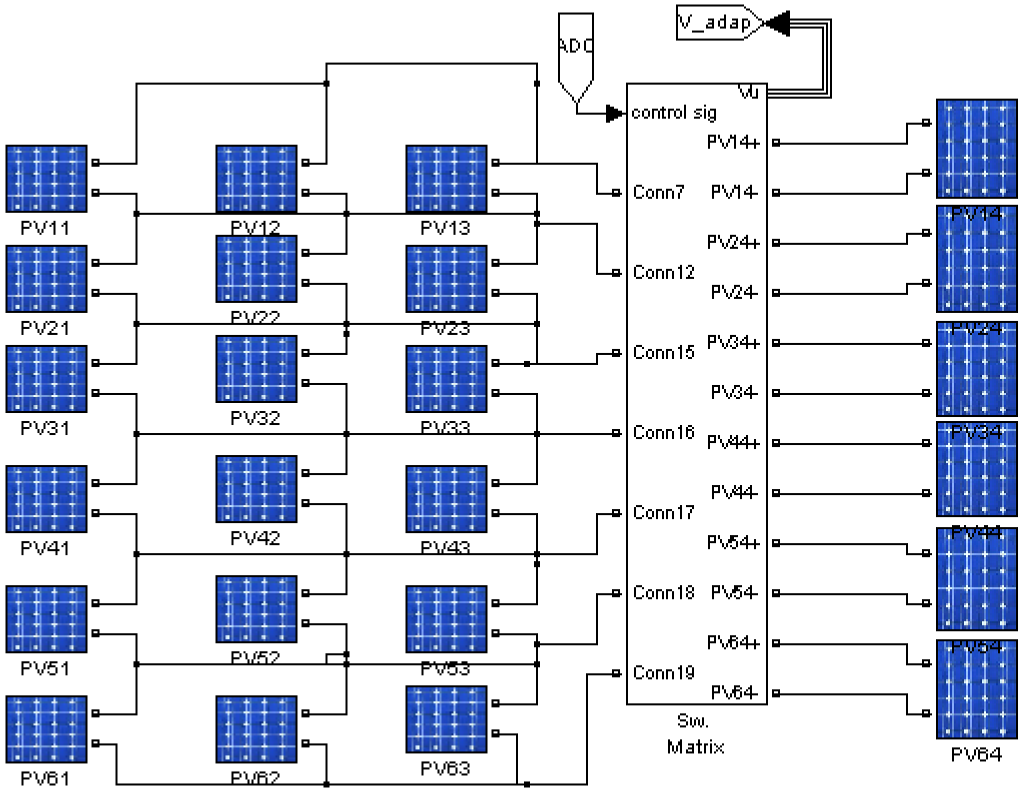

Figure 4.18: Simulation model of the adaptive bank

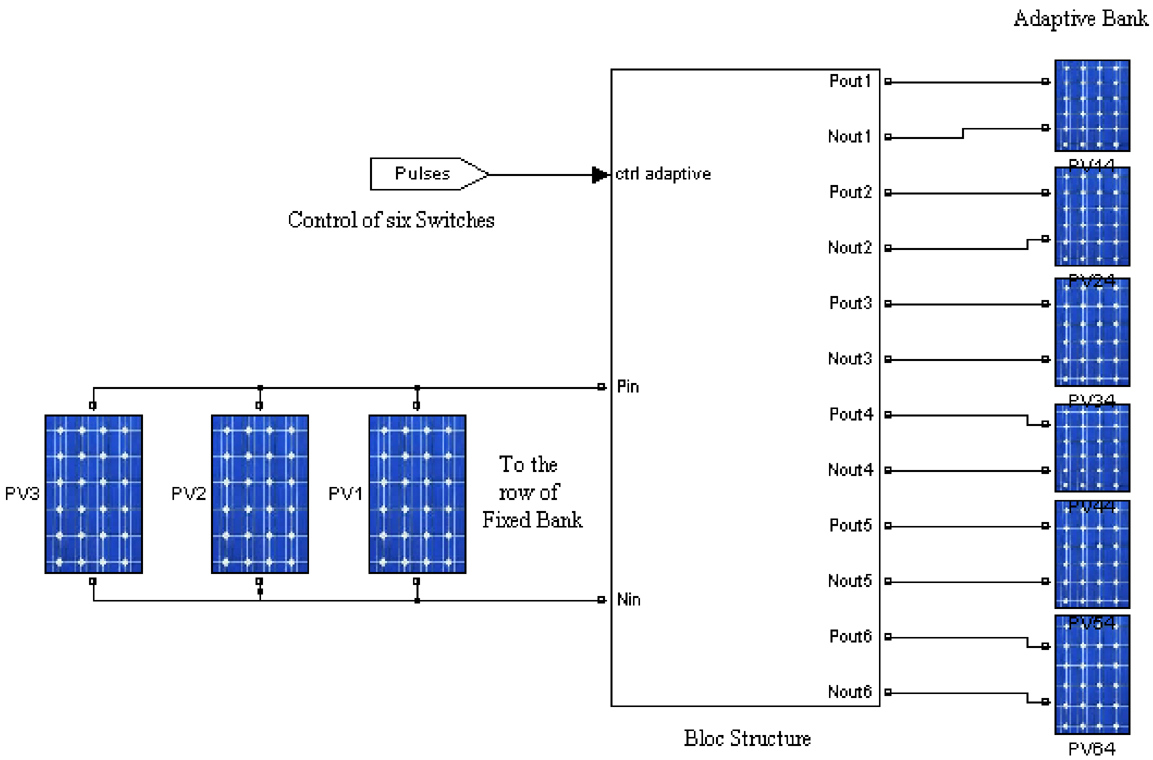

Figure 4.19: Structure of one bloc in the switching matrix

4.3.1 Simulation results of adaptive bank

Different partial shading configurations will be discussed in this part of the thesis. These configurations are going to be evaluated with and without the use of adaptive banking to examine the efficiency of the method.

4.3.2 First configuration

In this configuration, the illumination scheme of the system arrays is presented in the next table. The system power and current results before the use of adaptive reconfiguration are presented in Figure 4.20. The figure shows that the maximum obtainable power in this case is 3.47kW with the existence of three different maximum power points in the power curve. The existence of multiple maximum power points affects the function of MPPT devices.

Table 4.3: Irradiation scheme of the first configuration

500	500	500	500
500	500	500	1000
1000	1000	1000	1000
1000	1000	1000	1000
1000	1000	1000	1000
1000	1000	1000	1000

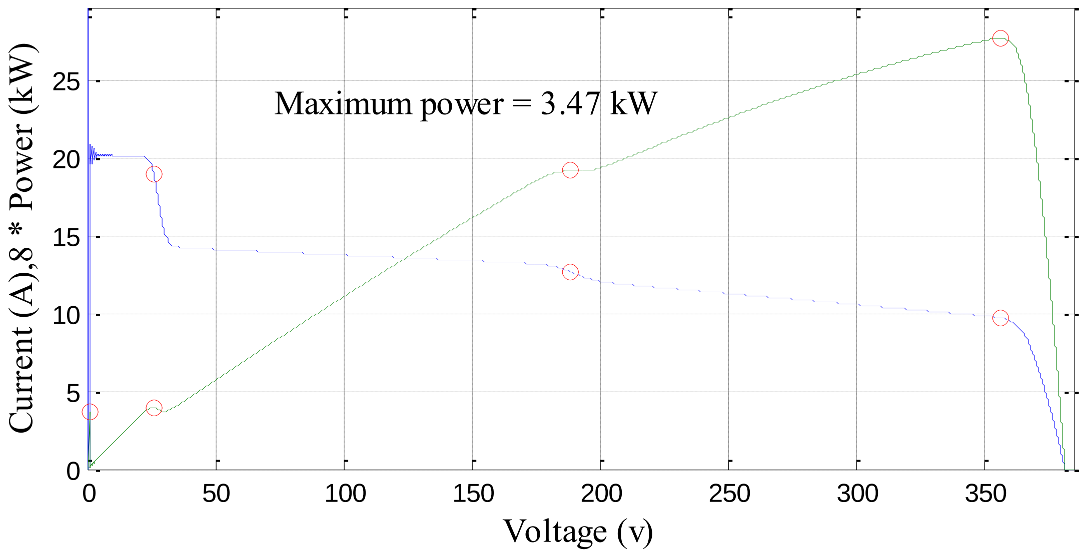

Figure 4.20: P-V and I-V curves without reconfiguration

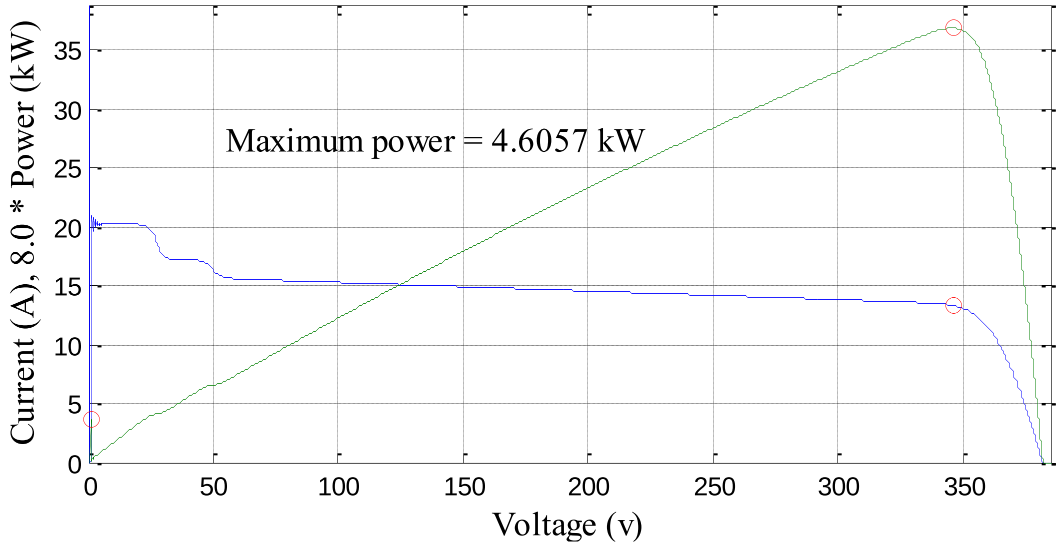

Figure 4.21: P-V and I-V curves after reconfiguration

The effect of multiple maximum points can lead the MPPT device to wrongly choose a local maximum point and consider it as the real maximum power point. Thus, it can lead the system to generate less power less than it can actually generate under same conditions.

Figure 4.21 presents the generated power of the system after the application of adaptive reconfiguration algorithm. From the first look we can notice that the power has risen to 4.6 kW instead of 3.47kW before the use of reconfiguration. The P-V curve is showing one maximum point which lead to better function of MPPT devices.

4.3.3 Second configuration

Table 4.4 presents the irradiation scheme in this configuration. Figure 4.22 shows the normally generated power out of the system with the absence of any reconfiguration algorithms. The figure shows that the maximum power that can be extracted from the system is 4.05kW.

Table 4.4: Irradiation scheme of the second configuration

300	500	1000	500
500	1000	1000	1000
500	1000	1000	200
500	1000	1000	1000
500	1000	1000	1000
1000	1000	1000	1000

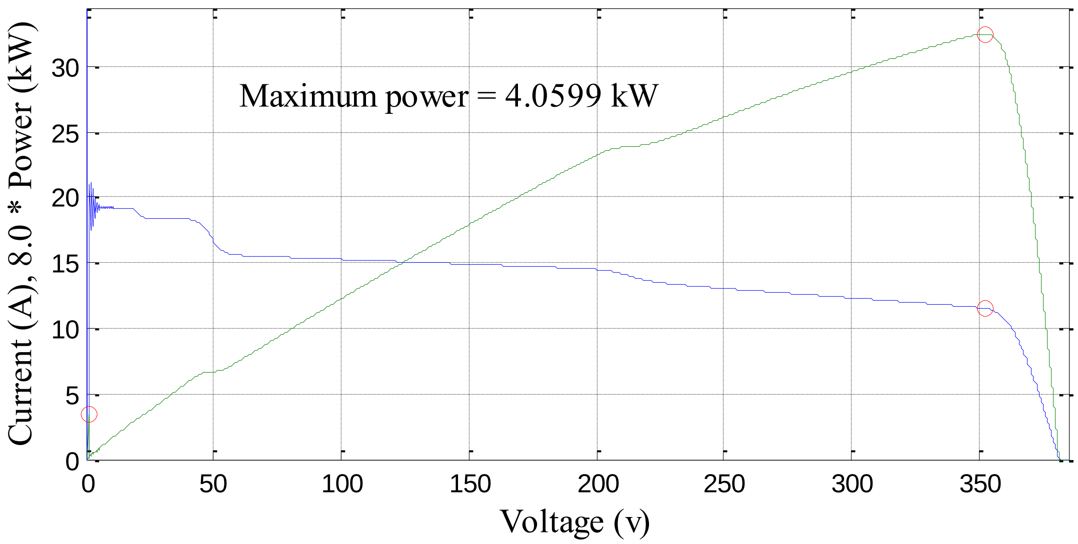

Figure 4.22: Power and current curves in the second scheme (without reconfiguration)

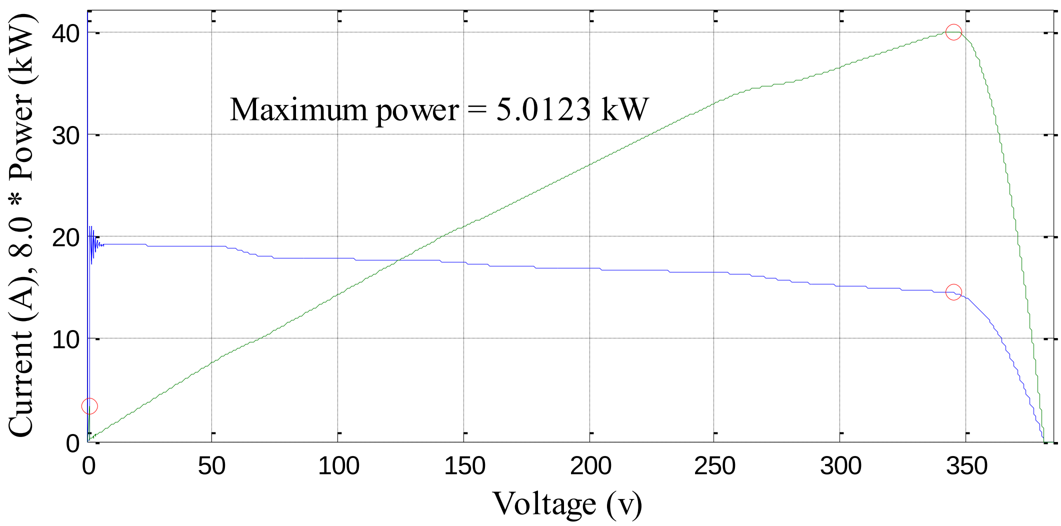

Figure 4.23: Power and Current of second scheme after using reconfiguration

After the implementation of reconfiguration algorithm, the power has increased from 4.05 to 5.01kW under the same irradiation parameters. The two curves in this case have one maximum power point and that doesn't affect the MPP tracker functions.

4.3.4 Third configuration

In this configuration, the solar array was irradiated as shown in Table 4.5. Triangular portion of the system was partially shaded to study the effect of this partial shading on the system. Different irradiation levels were applied as the table shows. The curves of the power and current as functions of the PV voltage are shown in **Figure 4.24**. The maximum power that can be extracted from the system under these conditions without reconfiguration was 4.12kW. However, after the use of reconfiguration algorithm based on the adaptive bank the maximum extracted power has increased to 5.21kW. This is demonstrated by the results of **Figure 4.25**. The power curve in this figure appears to be smooth when single maximum power point. The reconfiguration process has shown an important improvement in the efficiency of the system under partial shading conditions.

Table 4.5: Irradiation of the solar array, third configuration

1000	1000	1000	1000
1000	1000	1000	600
500	400	1000	1000
700	200	1000	1000
850	500	600	400
1000	1000	300	300

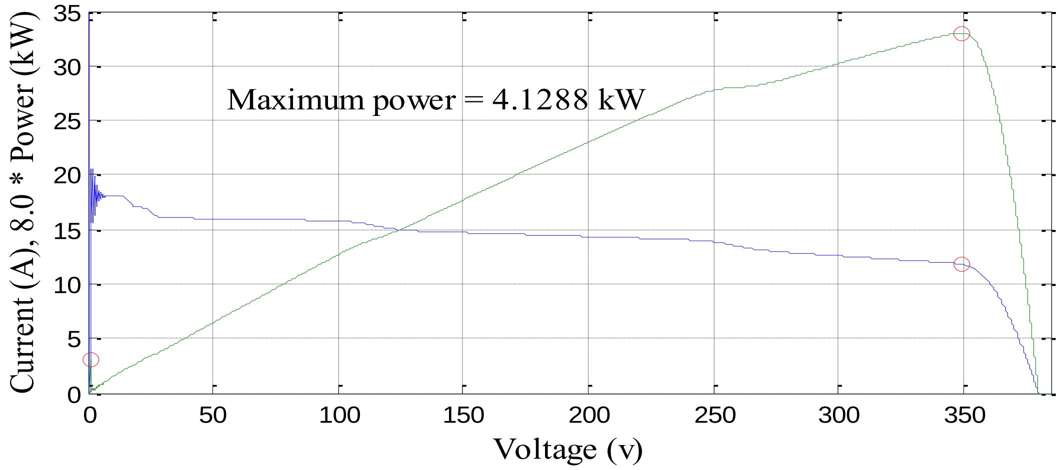

Figure 4.24: P-V and I-V curves without reconfiguration

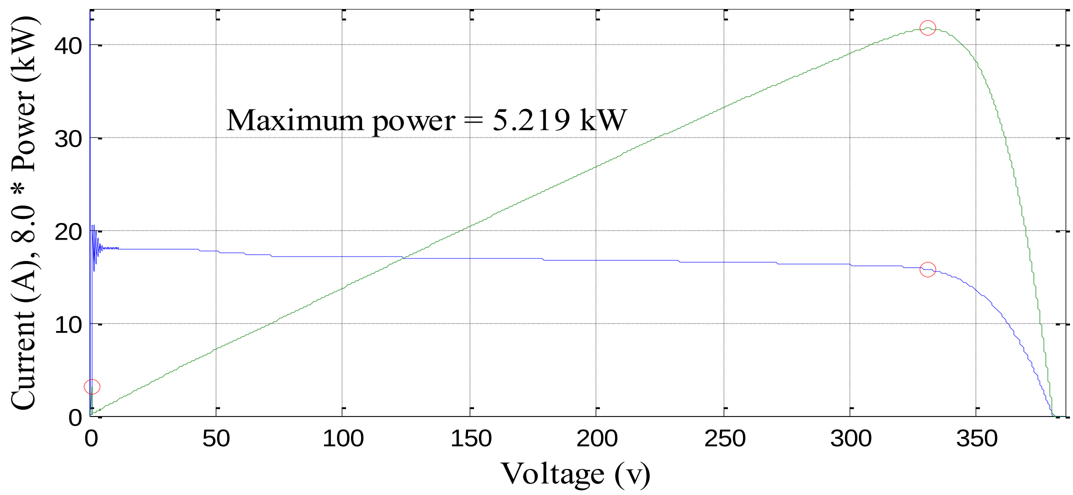

Figure 4.25: P-V and I-V curves after reconfiguration

4.4 Comparison of Different Structures

This chapter has focused on the use of different measures of overcoming the problem of partial shading in photovoltaic systems. Table 4.6 represents a brief comparison of the different methods including their main advantages and disadvantages. The table shows that the irradiance equalization algorithm is the best in terms of power generation and modules protection against hotspot effect. However, this algorithms complexity is increasing with the square of the number of modules in the system.

Table 4.6: Advantages and disadvantages of the different algorithms presented

Method	Advantages
SP connection	Simple, easy to implement, unable to overcome the partial shading and hotspot problems, low power generation at partial shading conditions
TCT connection	Needs more connections, easy to implement, has better performance in avoiding some partial shading cases, produce higher power than SP
Parallel diodes	Simple and easy to implement, Ability to avoid hotspot problem by bypassing the entire shaded module, cause significant power reduction if modules are shaded, cause the creation of multiple peak power points, affect the function of MPPT devices
Irradiance equalization	Complex implementation, high cost, highest performance under different partial shading parameters, higher power generation, cause no effects on MPPT devices
Adaptive banking (algorithm 1)	Less complex, less costly and simpler to implement than irradiance equalization, its performance is redundant and depends on the partial shading parameters, need less power switches and less sensors.
Adaptive banking (algorithm 2)	Less complex, less costly and simpler to implement than irradiance equalization, its performance is also redundant and depends on the partial shading parameters, need less power switches, needs more sensors to achieve its goal.

4.3.5 Conclusions

This work has discussed the problem of partial shading in solar systems and its effects on the function and efficiency of the solar generators. Problem of partial shading is common in small solar system used at homes or in residential areas where buildings and trees shadow can fall on the solar arrays. The problem of partial shading can cause different problems to the solar systems such as degradation of the efficiency of the solar panels. Shaded parts of the solar array can face the phenomena of hotspot because they will behave like loads for the other non-shaded elements. These shaded parts will consume the energy produced by other elements instead of generating electric power. The consumed power is dissipated in the shaded cells under form of heat that can destroy permanently the cells.

This work also has discussed the reconfiguration process in which the arrangement of different panels or cells in a solar array is applied to overcome the partial shading effects. This arrangement is achieved through the use of special switching matrix able to change the connections between different cells or panels of the system. Different reconfiguration algorithms and connection schemes of the solar system were presented and discussed throughout the work of this thesis. Simulation of different configurations and algorithms was carried out using the MATLAB software to study the efficiency of these algorithms in avoiding partial shading effects on the solar system. The obtained results have shown that the use of parallel diode is efficient in most of partial shading cases if compared to the use of different configurations. The implementation of TCT configuration has also partially come over the partial shading effects compared to the SP, HC, and BL connections.

The use of reconfiguration algorithms has shown good results increasing the efficiency of partial shaded solar systems. Two different reconfiguration algorithms were implemented and discussed in this work under different shading conditions. Simulation of these two algorithms has shown that the use of adaptive bank is efficient when the partial shading is affecting small number of elements. When the partial shading affects more elements this algorithm’s efficiency decreases. The electric adaptive reconfiguration EAR algorithm has shown more efficiency in term of increasing the efficiency of the shaded system. However, this system is costly in terms of the number of required switches.

REFERENCES

Balato, M., Costanzo, L., & Vitelli, M. (2015). Optimization of both the energetic efficiency and the duration of life of PV arrays by means of the dynamical reconfiguration of PV modules connections. *Tenth International Conference on Ecological Vehicles and Renewable Energies (EVER)* (pp. 1-6). Monte Carlo: IEEE. doi:10.1109/EVER.2015.7112922

Barron, A., & Chatelain, B. (2011, Oct). *Introduction to solar cell technology*. Retrieved May 2016, from Openstax cnx: https://cnx.org/contents/3QU3ovtd@1/An-Introduction-to-Solar-Cell-

Bowden, S., & Honsberg, C. (n.d.). *pvcdrom*. Retrieved 11 29, 2015, from pv education org: http://www.pveducation.org/pvcdrom/solar-cell-operation/iv-curve

Buddha, S. T. (2011). *Topology Reconfiguration To Improve The Photovoltaic (PV) Array Performance.* Arizona State University.

Buddha, S. T. (2011). *Topology Reconfiguration To Improve The Photovoltaic (PV) Array Performance.* ARIZONA STATE UNIVERSITY.

Candela, R., Dio, V. d., Sanseverino, E. R., & Romano, P. (2007). Reconfiguration Techniques of Partial Shaded PV Systems for the Maximization of Electrical Energy Production. *2007 International Conference on Clean Electrical Power* (pp. 716-719). IEEE. doi:10.1109/ICCEP.2007.384290

Chaaban, M. A. (2011). *Adaptive Photovoltaic Configurations For Decreasing The Electrical Mismatching Losses, MSc thesis.* University of Nebraska-Lincoln .

Chaw, C. L. (2015). *An Approach to Reduce the Effect of Partial Shading on Photovoltaic Modules, MSc. Thesis.* University of British Columbia.

Cheng, Z., Pang, Z., Liu, Y., & Xue, P. (2010). An adaptive solar photovoltaic array reconfiguration method based on fuzzy control. *8th World Congress on Intelligent Control and Automation (WCICA)* (pp. 176-181). Jinan: IEEE. doi:10.1109/WCICA.2010.5553911

Cipriani, G., Dio, V. D., Madonia, N., Miceli, R., Pellitteri, F., & Galluzzo, F. R. (2014). Reconfiguration Strategies to Reduce Mismatch Effects on PV Array: an Arduino Based Prototype. *International Symposium on Power Electronics, Electrical Drives, Automation and Motion* (pp. 1003-1008). IEEE.

El-Dein, M. Z., Kazerani, M., & Salama, M. M. (2013). Optimal Photovoltaic Array Reconfiguration to Reduce Partial Shading Losses. *IEEE Transactions on Sustainable Energy, 4*(1), 145-153. doi:10.1109/TSTE.2012.2208128

EL-Moghany, M. S. (2011). Sun and Maximum Power Point Tracking in Solar Array Systems Using Fuzzy Controllers Via FPGA. Gaza, The Islamic University, Palestine.

Fife, M. (2010). *Solar Power Reliability and Balance-of-System Designs*. Retrieved 11 29, 2016, from Renewable Energy World: http://www.renewableenergyworld.com/articles/print/rewna/volume-2/issue-5/solar-energy/solar-power-reliability-and-balance-of-system-designs.html

Guillermo, V.-Q., Francisco, G.-G., Robert, P.-L., Manuel, R.-L., & Alfonso, C.-R. (2009). Electrical PV Array Reconfiguration Strategy for Energy Extraction Improvement in Grid-Connected PV Systems. *IEEE Transactions on Industrial Electronics, 56*(11), 4319-4331. doi:10.1109/TIE.2009.2024664

Inc, A. L. (2015). *Mono-crystalline*. Retrieved 12 15, 2015, from solar-facts-and-advice: http://www.solar-facts-and-advice.com/monocrystalline.html

Karakose, M., Baygin, M., Baygin, N., Murat, K., & Akin, E. (2014). An Intelligent Reconfiguration Approach Based on Fuzzy Partitioning in PV Arrays. *IEEE*.

Karaköse, M., Murat, K., Akın, E., & Parlak, K. S. (2014). A New Efficient Reconfiguration Approach Based on Genetic Algorithm in PV Systems. *IEEE 23rd International Symposium on Industrial Electronics* (pp. 23-28). IEEE.

Lehman, B., & Nguyen, D. (2008). A reconfigurable solar photovoltaic array under shadow conditions. *Applied Power Electronics Conference and Exposition, 2008* (pp. 980 - 986). Austin, TX: IEEE. doi:10.1109/APEC.2008.4522840

Liedholm, E. (2010). *Tracking the maximum power point, MSc. thesis.* Chalmers University of Technology.

Lin, X., Wang, Y., Yue, S., Shin, D., Chang, N., & Pedram, M. (2012). Near-Optimal, Dynamic Module Reconfiguration in a Photovoltaic System to Combat Partial Shading Effects. *DAC2012.* San Francisco, California, USA.

Linvents. (2015). *Solar Photovoltaic Technologies*. Retrieved Jun 2016, from solar building technologies: http://www.solarbuildingtech.com/Solar_PV_Tech/solar_photovoltaic_technologies.htm

Manna, D. L., Vigni, V. L., Sanseverino, E. R., Dio, V. D., & Romano, P. (2014). Reconfigurable Electrical Interconnection Strategies for Photovoltaic Arrays: a Review. *Renewable and Sustainable Energy Reviews, Elsevier*, 412-426.

Morales, D. S. (2010). *Maximum Power Point Tracking Algorithms for Photovoltaic Applications.* Aalto university.

Moring, S., & Pols, A. (2012). *Maximum Power Point Tracking: Algorithm and Software Development.* Delft university of technology.

Motaleb, A. M. (2010). *Maximum Power Point Tracking in photovoltaic systems.* Sevilla: Universidad de Sevilla.

Nguyen, D., & Lehman, B. (2008). A Reconfigurable Solar Photovoltaic Array Under Shadow Conditions. *IEEE* (pp. 980-986). Northeastern University, Boston.

Nguyen, D., & Lehman, B. (2008). A Reconfigurable Solar Photovoltaic Array Under Shadow Conditions. *IEEE*, 980-986.

Nguyen, D., & Lehman, B. (2008). An Adaptive Solar Photovoltaic Array Using Model-Based Reconfiguration Algorithm. *IEEE Transactions on Industrial Electronics, 55*(7), 2644 - 2654. doi:10.1109/TIE.2008.924169

Parlak, K. Ş. (2013). A New reconfiguration method for PV array system. *Industrial Electronics Society, IECON 2013 - 39th Annual Conference of the IEEE* (pp. 1478 - 1483). Vienna: IEEE. doi:10.1109/IECON.2013.6699351

Romano, P., Candela, R., Cardinale, M., Vigni, V. L., Musso, D., & Sanseverino, E. R. (2013). Optimization of Photovoltaic Energy Production through an Efficient Switching Matrix. *Journal of Sustainable Development of Energy, Water and Environment Systems, 1*(3), 227-236.

Romano, P., Candela, R., Cardinale, M., Vigni, V. L., Musso, D., & Sanseverino, E. R. (2013). Optimization of Photovoltaic Energy Production through an Efficient Switching Matrix. *Journal of Sustainable Development of Energy, Water and Environment Systems, 1*(3), 227-236. doi:10.13044/j.sdewes.2013.01.0017

Serna-Garcés, S. I., Bastidas-Rodríguez, J. D., & Ramos-Paja, C. A. (2016, 2 9). Reconfiguration of Urban Photovoltaic Arrays Using Commercial Devices. *energies*, pp. 1-23.

Shaaban, M. A. (2011). *Adaptive Photovoltaic configurations for Decreasing the Electrical Mismatching losses, MSc.* University of Nebraska-Lincoln.

Shams El-Dein, M. Z. (2012). *Novel Designs for Photovoltaic Arrays to Reduce Partial Shading Losses and to Ease Series Arc Fault Detection, PhD.* University of Waterloo.

Solar Micro Inverter, Enphase. (2016, 03 17). Retrieved from https://enphase.com/en-us

Storey, J. P., Wilson, P. R., & Bagnall, D. (2013). Improved Optimization Strategy for Irradiance Equalization in Dynamic Photovoltaic Arrays. *IEEE Transactions on Power Electronics, 28*(6), 2946 - 2956. doi:10.1109/TPEL.2012.2221481

Velasco, G., Guinjoan, F., & Pique, R. (2008). Grid-connected PV systems energy extraction improvement by means of an Electric Array Reconfiguration (EAR) strategy: Operating principle and experimental results. *2008 IEEE Power Electronics Specialists Conference* (pp. 1983 - 1988). Rhodes: IEEE. doi:10.1109/PESC.2008.4592234

Velasco, G., Guinjoan, F., & Piqué, R. (2014). Grid-Connected PV Systems Energy Extraction Improvement by means of an Electric Array Reconfiguration (EAR) Strategy: Operating Principle and Experimental Results. *IEEE*, 1983-1988.

Vilela, A. o., Oliveira, J. H., Ribeiro, G. A., Brandao, A. S., & Pereira, H. A. (2011). Switching Reconfiguration of a Solar Photovoltaic Converter Considering Shadow Conditions. *IEEE*, (pp. 1143-1147).

Villalva, M. G., Gazoli, J. R., & Filho, E. R. (2009). Comprehensive Approach to Modeling and Simulation of Photovoltaic Arrays. *IEEE TRANSACTIONS ON POWER ELECTRONICS. 24*, pp. 1198-1208. IEEE. Retrieved 4 3, 2016

Villalva, M. G., Gazoli, J. R., & Ruppert, E. (2009). Modeling and circuit based simulation of photovoltaic arrays. *Brazilian journal of power electronics, 14*(1), 35-45.

Xuejun, L. (2004). *An improved perturbation and observation maximum power point tracking algorithm for PV panels.* Concordia university.

Zhang, Q. (2011). *MAXIMUM POWER POINT TRACKING IN PHOTOVOLTAIC SYSTEMS USING MODEL REFERENCE ADAPTIVE CONTROL.* China: Shanghai Jiao Tong University.

APPENDIX

Parameters of the simulated solar panel SPR-300-WHT from SUNPOWER

Nominal Power	300W
Maximum power point voltage	54.7V
Maximum power point current	5.49A
Open circuit voltage	64V
Short circuit current	5.87A